



# Provably Tightest Linear Approximation for Robustness Verification of Sigmoid-like Neural Networks

Zhaodi Zhang  
zdzhang@stu.ecnu.edu.cn  
East China Normal University  
Shanghai, China

Yiting Wu  
51205902026@stu.ecnu.edu.cn  
East China Normal University  
Shanghai, China

Si Liu  
si.liu@inf.ethz.ch  
ETH Zürich  
Zürich, Switzerland

Jing Liu  
jliu@sei.ecnu.edu.cn  
Shanghai Key Laboratory of  
Trustworthy Computing,  
East China Normal University  
Shanghai, China

Min Zhang  
zhangmin@sei.ecnu.edu.cn  
East China Normal University,  
Shanghai Institute of Intelligent  
Science and Technology  
Shanghai, China

## ABSTRACT

The robustness of deep neural networks is crucial to modern AI-enabled systems and should be formally verified. Sigmoid-like neural networks have been adopted in a wide range of applications. Due to their non-linearity, Sigmoid-like activation functions are usually *over-approximated* for efficient verification, which inevitably introduces imprecision. Considerable efforts have been devoted to finding the so-called *tighter* approximations to obtain more precise verification results. However, existing tightness definitions are heuristic and lack theoretical foundations. We conduct a thorough empirical analysis of existing *neuron-wise* characterizations of tightness and reveal that they are superior only on specific neural networks. We then introduce the notion of *network-wise tightness* as a unified tightness definition and show that computing network-wise tightness is a complex non-convex optimization problem. We bypass the complexity from different perspectives via two efficient, provably tightest approximations. The results demonstrate the promising performance achievement of our approaches over state of the art: (i) achieving up to 251.28% improvement to certified lower robustness bounds; and (ii) exhibiting notably more precise verification results on convolutional networks.

## CCS CONCEPTS

• **Software and its engineering** → *Formal software verification*; • **Theory of computation** → *Abstraction*.

### ACM Reference Format:

Zhaodi Zhang, Yiting Wu, Si Liu, Jing Liu, and Min Zhang. 2022. Provably Tightest Linear Approximation for Robustness Verification of Sigmoid-like Neural Networks. In *37th IEEE/ACM International Conference on Automated*

Permission to make digital or hard copies of all or part of this work for personal or classroom use is granted without fee provided that copies are not made or distributed for profit or commercial advantage and that copies bear this notice and the full citation on the first page. Copyrights for components of this work owned by others than ACM must be honored. Abstracting with credit is permitted. To copy otherwise, or republish, to post on servers or to redistribute to lists, requires prior specific permission and/or a fee. Request permissions from [permissions@acm.org](mailto:permissions@acm.org).

ASE '22, October 10–14, 2022, Rochester, MI, USA

© 2022 Association for Computing Machinery.

ACM ISBN 978-1-4503-9475-8/22/10...\$15.00

<https://doi.org/10.1145/3551349.3556907>

*Software Engineering (ASE '22), October 10–14, 2022, Rochester, MI, USA. ACM, New York, NY, USA, 13 pages. <https://doi.org/10.1145/3551349.3556907>*

## 1 INTRODUCTION

The reliability concerns about deep neural networks (DNNs) are increasing more drastically than ever, especially as such networks are being embedded into software systems to make them intelligent. Considerable efforts from both AI and software engineering communities have been devoted to achieving *robust* DNNs by leveraging testing and verification techniques [4, 12, 32, 40, 42, 47, 48, 54]. Among these attempts, formal methods have been demonstrated effective in offering certified robustness guarantees, giving birth to an emerging research field called *Trustworthy AI* [50]. One distinguishing feature of formal methods is that they could provide rigorous proofs of correctness automatically when the properties are satisfied or disprove them by counterexamples (i.e., witnesses to the violations) [3, 9]. Robustness is an important correctness property in DNN verification: Minor modifications to the neural network's inputs must *not* alter its outputs [7]. Guaranteeing robustness is indispensable to prevent AI-enabled systems from environmental perturbations and adversarial attacks.

Formal robustness verification of DNNs has been well studied in recent years [14, 16, 20, 32, 33, 42, 45, 47–49]. Most efforts are focused on the *ReLU networks* that only use the simple piecewise ReLU activation function. Despite their wide adoptions in modern AI-enabled systems, another notable class of S-shaped (or Sigmoid-like) activation functions, such as Sigmoid, Tanh, and Arctan, have not attracted much attention yet. Due to their non-linearity, Sigmoid-like activation functions are far more complex to be verified. A *de facto* solution is to over-approximate such functions by linear bounds and to transform the verification problem into efficiently solvable linear programming. Many state-of-the-art DNN verification techniques, e.g., abstract interpretation [16, 40], symbolic interval propagation [45], model checking [33], differential verification [32], reachability and output range analysis [13, 44], are based on linear approximation.

Over-approximation inevitably introduces imprecision, rendering approximation-based verification incomplete: *Unknown* results

may be returned when the neural network’s robustness cannot be verified. Considerable efforts have been devoted to finding the so-called *tighter* approximations to achieve more precise verification results. For example, a larger certified lower robust bound [5, 28] (the perturbation distance under which a neural network is proved robust against any allowable perturbation) is preferable in approximation. Several characterizations of tightness and approximation approaches have been proposed for Sigmoid-like activation functions [5, 18, 26, 28, 51, 55]. However, they are all heuristic and lack theoretical foundations for the individual outperformance.

We conduct a thorough empirical analysis of existing approaches and reveal that they are superior only on specific neural networks. In particular, we have found that the claimed tighter approximation actually produces smaller certified lower bounds according to the tightness defined and observed frequent occurrences of such cases.

Motivated by these observations, we introduce the notion of *network-wise tightness* as a *unified* tightness definition to characterize linear approximations of Sigmoid-like activation functions. This new definition ensures that a tighter approximation can always compute larger certified lower bounds (i.e., larger safe radius). However, we show that it unfortunately implies that computing the tightest approximation is essentially a network-wise non-convex optimization problem [28], which is hard to solve in practice [31].

We bypass the complex optimization problem from two different perspectives, depending on the neural network architecture. For the networks *with only one hidden layer*, we leverage a gradient-based searching algorithm for computing the tightest approximations. Regarding the networks *with multiple hidden layers*, based on our empirically study of the state-of-the-art tools, we have gained an insight that *a larger robust bound can be computed when the intervals keep to be tighter during the layer-by-layer propagation*. Based on this insight, we propose a *neuron-wise* tightest approximation and prove that it guarantees the *network-wise tightest approximation* when the networks are of non-negative weights. Such networks have been demonstrated suitable in a wide range of applications such as effective defense for adversarial attacks in malware and spam detection [8, 15, 19] and balancing accuracy and robustness in autoencoding [1, 29].

We have implemented a prototype of our approach called `NeWise`<sup>1</sup> and extensively compared it to three state-of-the-art tools, namely `DEEPCERT` [51], `VERINET` [18], and `ROBUSTVERIFIER` [26]. Our experimental results show that `NeWise` (i) achieves up to 251.28% improvement to certified lower robustness bounds in the provably tightest cases and (ii) exhibits up to 122.22% improvement to certified lower robustness bounds on convolutional networks.

To summarize, this paper makes three major contributions:

- (1) We have introduced a novel unified definition of *network-wise tightness* to characterize the tightness of linear approximations for neural network robustness verification.
- (2) We have identified two cases where we can efficiently achieve provably tightest approximations; the corresponding approaches have been proposed.
- (3) We have implemented a verification tool and conducted comprehensive evaluation on its effectiveness and efficiency over three state-of-the-art verifiers.

<sup>1</sup>Our code is available at <https://github.com/FormalAIze/NeWise.git>.

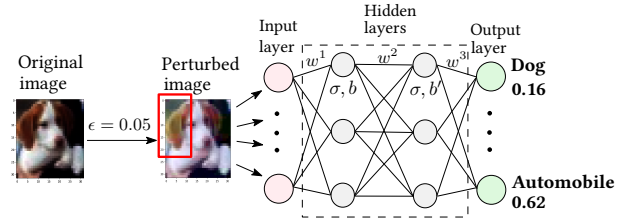


**Figure 1: A perturbed image of a dog is misclassified to an automobile with 62% probability in 0.05 perturbation radius.**

The remainder of this paper proceeds as follows: Section 2 gives preliminaries on robustness verification of neural networks. Section 3 shows the tightness measurements of linear approximations and introduce our notion of network-wise tightness. Sections 4 and 5 present our provably tightest approximations from two different perspectives, respectively. Section 6 describes our evaluation results. We discuss related work in Section 7 and conclude in Section 8.

## 2 PRELIMINARIES

### 2.1 Robustness Verification of Neural Networks

**2.1.1 Deep Neural Network.** A deep neural network is a directed network, where the nodes are called neurons and arranged layer by layer. Each neuron is associated with an activation function  $\sigma(x)$  and a bias  $b$ . Except for the first layer, the neurons on a layer are connected to those on the preceding layer, as shown in Figure 1. Every edge is associated with a weight, which is computed by training. The first and last layers are called input and output layers, respectively. The others between them are called hidden layers.

The *execution* of a neural network follows the style of layer-by-layer propagation. Each neuron on the input layer admits a number. The number is multiplied by the weights on the edges and then passed to the successor neurons on the next layer. All the incoming numbers are summed. The summation is fed to the activation function  $\sigma$  and the output of  $\sigma$  is added with the bias  $b$ . The result is then propagated to the next layer until reaching the output layer.

Formally, a  $k$ -layer neural network is a function  $f: \mathbb{R}^n \rightarrow \mathbb{R}^m$  of the form  $f^k \circ \sigma^{k-1} \circ \dots \circ \sigma^1 \circ f^1$ , with  $\sigma^t$  being a non-linear and differentiable activation function for  $t$ -th layer. The function  $f^t$  is either an affine transformation *or* a convolutional operation:

$$f(x) = Wx + b, \quad (\text{Affine Transformation})$$

$$f(x) = W * x + b, \quad (\text{Convolutional Operation})$$

where  $W$ ,  $b$ , and  $*$  refer to the weight matrix, the bias vector, and the convolutional product, respectively. In this work, we focus on the networks with the Sigmoid-like activation functions i.e., Sigmoid, Tanh, and Arctan, which are defined as follows, respectively.

$$\sigma(x) = \frac{1}{1 + e^{-x}}, \quad \sigma(x) = \frac{e^x - e^{-x}}{e^x + e^{-x}}, \quad \sigma(x) = \tan^{-1}(x)$$

The output of a neural network  $f$  is a vector of  $m$  floating numbers between 0 and 1, denoting the probabilities of classifying an input to the  $m$  labels. Let  $S$  be the set of  $m$  classification labels for the network  $f$ . We use  $\mathcal{L}(f(x))$  to represent the output label for

the input  $x$  with

$$\mathcal{L}(f(x)) = \arg \max_{s \in S} f(x)[s].$$

Intuitively,  $\mathcal{L}(f(x))$  returns a label  $s$  in  $S$  such that  $f(x)[s]$  is maximal among the numbers in the output vector.

**2.1.2 Robustness and Robustness Verification.** Neural networks are essentially “programs” composed by computers by fine-tuning the weights in the networks from training data. Unlike the handcrafted programs developed by programmers, neural networks lack formal requirements and are almost inexplicable, making it very challenging to formalize and verify their properties.

A neural network is called *robust* if reasonable perturbations to its inputs do not alter the classification result. A perturbation is typically measured by the distance between the perturbed input  $x'$  and the original one  $x$  by using  $\ell_p$ -norm, denoted by  $\|x - x'\|_p \triangleq \sqrt[p]{|x_1 - x'_1|^p + \dots + |x_n - x'_n|^p}$ , where  $p$  can be 1, 2 or  $\infty$ , and  $n$  is the length of the vectors  $x$ . In this work, we consider the most general case when  $p = \infty$ .

**Example 1.** We consider an example to explain how a perturbed image is misclassified. As shown in Figure 1, a normal image of a dog can be correctly classified by a neural network. We assume that the image can be perturbed within a 0.05 distance under  $\ell_\infty$ -norm. There exists a perturbed image such that when it is fed into the network, the outputs of the two neurons labeled by *dog* and *automobile* are 0.16 and 0.62, respectively. It indicates that the image is classified to a dog (resp. automobile) with the probability of 16% (reps. 62%). Therefore, it is classified to be an automobile, although it still represents a dog to human eyes, apparently.

The robustness of a neural network can be quantitatively measured by a lower bound  $\epsilon$ , which refers to a safe perturbation distance such that any perturbations below  $\epsilon$  have the same classification result as the original input to the neural network.

**DEFINITION 1 (LOCAL ROBUSTNESS).** Given a neural network  $f$ , an input  $x_0$ , and a bound  $\epsilon$  under  $\ell_p$ -norm,  $f$  is called *robust* w.r.t.  $x_0$  iff  $\mathcal{L}(f(x)) = \mathcal{L}(f(x_0))$  holds for each  $x$  such that  $\|x - x_0\|_p \leq \epsilon$ . Such  $\epsilon$  is called a *certified lower bound*.

The twin problems of verifying  $f$ 's robustness are: (i) to prove that, for each  $x$  satisfying  $\|x - x_0\|_p \leq \epsilon$ ,

$$f_{s_0}(x) - f_s(x) > 0 \quad (1)$$

holds for each  $s \in S - \{s_0\}$ , where  $s_0 = \mathcal{L}(f(x_0))$  and  $f_s(x)$  returns the probability, i.e.,  $P(\mathcal{L}(f(x)) = s)$ , of classifying  $x$  to the label  $s$  by  $f$ ; and (ii) to compute a certified lower bound – a larger certified lower bound implies a more precise robustness verification result. As directly computing  $\epsilon$  is difficult due to the non-linearity of the constraint (1), most of the state-of-the-art approaches [5, 51, 55] adopt the efficient binary search algorithm to first determine a candidate  $\epsilon$  and then check whether (1) is true or false on  $\epsilon$ .

## 2.2 Approximation-based Robustness Verification

A neural network  $f$  is highly non-linear due to the inclusion of activation functions. Proving Formula (1) is computationally expensive, e.g., NP-complete even for the simplest fully connected ReLU networks [20, 37]. Many approaches have been investigated to

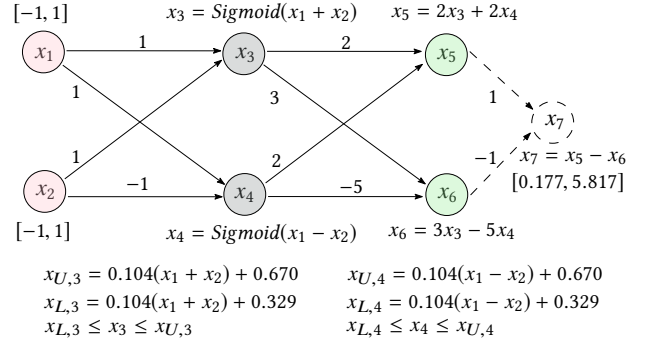


**Figure 2: An example of approximation-based verification.**

improve the verification efficiency while sacrificing completeness. Representative methods include interval analysis [46], abstract interpretation [16, 40], and output range estimation [13, 52], etc. The technique underlying these approaches is to over-approximate the non-linear activation functions using linear constraints, which can be more efficiently solved than the original ones.

Instead of directly proving Formula (1), the approximation-based approaches over-approximate both  $f_{s_0}(x)$  and  $f_s(x)$  by two linear constraints and prove that the lower linear bound  $f_{L,s_0}(x)$  of  $f_{s_0}(x)$  is greater than the upper linear bound  $f_{U,s}(x)$  of  $f_s(x)$ . Apparently,  $f_{L,s_0}(x) - f_{U,s}(x) > 0$  is a sufficient condition of Formula (1), and it is significantly more efficient to prove or disprove. Therefore, it is widely adopted in neural network verification [5, 18, 26, 51], although it may produce false positives when it is disproved.

**DEFINITION 2 (UPPER/LOWER LINEAR BOUNDS).** Let  $\sigma(x)$  be a non-linear function with  $x \in [l, u]$ ,  $\alpha_L, \alpha_U, \beta_L, \beta_U \in \mathbb{R}$ , and

$$h_U(x) = \alpha_U x + \beta_U, \quad h_L(x) = \alpha_L x + \beta_L. \quad (2)$$

$h_U(x)$  and  $h_L(x)$  are called *upper and lower linear bounds* of  $\sigma(x)$  if the following condition holds:

$$\forall x \in [l, u], \quad h_L(x) \leq \sigma(x) \leq h_U(x). \quad (3)$$

Over-approximating the non-linear activation functions using linear lower and upper bounds is the key to the approximation of a neural network. For each activation function  $\sigma$  on a domain  $[l, u]$ , we define an upper linear bound  $h_U$  and a lower one  $h_L$  to ensure that for all  $x$  in  $[l, u]$ ,  $\sigma(x)$  is enclosed in  $[h_L(x), h_U(x)]$ .

Given an input range as in Definition 1, the output ranges of a network are computed by propagating the output interval of each neuron as in Definition 2 to the output layer.

**Example 2.** We consider an example of verifying a simple neural network based on approximation, as shown in Figure 2. The original verification problem is to prove that for any input  $(x_1, x_2)$  with  $x_1 \in [-1, 1]$  and  $x_2 \in [-1, 1]$ , it is always classified to the label of neuron  $x_5$ . That is equivalent to proving that the output of the auxiliary neuron  $x_7 = (x_5 - x_6)$  is always greater than 0. We define the linear upper/lower bounds  $x_{U,3}, x_{L,3}$  and  $x_{U,4}, x_{L,4}$  to over-approximate  $x_3$  and  $x_4$ , respectively. It suffices to prove that  $x_{L,5} - x_{U,6} > 0$  is always true. We can over-estimate the output interval of  $x_{L,5} - x_{U,6}$  is  $[0.177, 5.817]$  using  $x_{U,3}, x_{L,3}$  and  $x_{U,4}, x_{L,4}$  and consequently prove the robustness of the network for all the inputs in  $[-1, 1] \times [-1, 1]$ .

Note that it is not necessary to approximate an activation function using only one linear upper or lower bound. One may consider

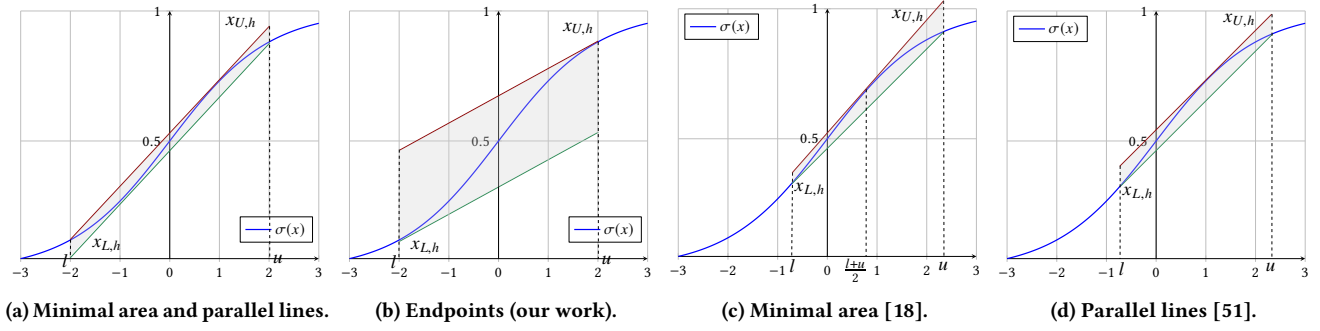


Figure 3: Different approximations according to the domain of  $\sigma(x)$  and their tightness definitions.

piece-wise linear bounds made up of a sequence of linear segments to approximate the function more tightly by being closer to it. However, the piece-wise way causes the number of constraints to blow up exponentially when propagated layer by layer [40]. It would drastically reduce the verification scalability. Thus, over-approximating an activation function using one upper linear bound and one lower linear bound is the most efficient and widely-adopted choice for the approximation-based robustness verification approaches.

### 3 LINEAR APPROXIMATION APPROACHES

In this section, we analyze the tightness issue of existing approximation approaches and formally define a unified network-wise tightness to characterize the approximations. The network-wise tightness guarantees that output neurons can produce precise output ranges.

#### 3.1 The Tightness Issue of Approximations

As approximation inevitably introduces overestimation, defining the *tightest* possible approximation is crucial to obtaining precise verification results. Several approximation approaches have been proposed under different strategies.

Henriksen et al. [18] proposed to measure the tightness of approximations using the enclosed area between the bound and the approximated function. An approximation is tighter if the corresponding area is smaller than another. By this definition, the approximations to  $x_3, x_4$  should be the following linear bounds:

$$x'_{U,3} = 0.204(x_1 + x_2) + 0.527, \quad (4)$$

$$x'_{L,3} = 0.204(x_1 + x_2) + 0.472, \quad (5)$$

$$x'_{U,4} = 0.204(x_1 - x_2) + 0.527, \quad (6)$$

$$x'_{L,4} = 0.204(x_1 - x_2) + 0.472. \quad (7)$$

Figure 3a shows the bounds graphically. Apparently, they are closer to the activation function on the interval  $[-2, 2]$ . Surprisingly, using the *tighter* linear bounds the output range of  $x_7$  is  $[-0.079, 6.073]$ , by which we cannot prove and disprove the robustness. Wu and Zhang adopted the same strategy for this case in their recent work [51]. In Example 2, we adopt a new strategy by taking the tangent lines at the two endpoints as its upper and lower bounds, as shown in Figure 3b. We obtain a smaller output range by these bounds, although they are far less tight than the one in Figure 3a.

In another case shown in Figure 3c, Henriksen et al. [18] proved that the tangent line at the middle point when  $x = \frac{l+u}{2}$  is the

Table 1: Tightness evaluation of state of the art: DEEPCERT[51], VERINET[28], and ROBUSTVERIFIER[26].  $\text{CNN}_{t-c}$  denotes a CNN with  $t$  layers and  $c$  filters of size  $3 \times 3$ . The models are pre-trained [2, 40, 51] by, e.g., DEEPPOLY [40].

| Dataset            | Model              | #Neurons | Certified Lower Bound (Average) |         |          |
|--------------------|--------------------|----------|---------------------------------|---------|----------|
|                    |                    |          | DEEPCERT                        | VERINET | ROB.VER. |
| MNIST              | 3x50               | 160      | 0.0076                          | 0.0077  | 0.0065   |
|                    | 3x100              | 310      | 0.0086                          | 0.0087  | 0.0074   |
|                    | 3x200              | 610      | 0.0091                          | 0.0092  | 0.0079   |
|                    | 5x100              | 510      | 0.0061                          | 0.0062  | 0.0052   |
|                    | 6x500              | 3,010    | 0.0778                          | 0.0776  | 0.0665   |
|                    | CNN <sub>3-2</sub> | 2,514    | 0.0579                          | 0.0580  | 0.0569   |
|                    | CNN <sub>3-4</sub> | 5,018    | 0.0473                          | 0.0472  | 0.0464   |
|                    | CNN <sub>4-5</sub> | 8,680    | 0.0539                          | 0.0543  | 0.0522   |
|                    | CNN <sub>5-5</sub> | 10,680   | 0.0548                          | 0.0550  | 0.0513   |
| CNN <sub>6-5</sub> | 12,300             | 0.0590   | 0.0588                          | 0.0541  |          |
| CNN <sub>8-5</sub> | 14,570             | 0.0878   | 0.0882                          | 0.0685  |          |
| Fashion MNIST      | 3x50               | 160      | 0.0101                          | 0.0102  | 0.0086   |
|                    | 5x100              | 510      | 0.0078                          | 0.0079  | 0.0066   |
|                    | CNN <sub>4-5</sub> | 8,680    | 0.0721                          | 0.0720  | 0.0666   |
|                    | CNN <sub>5-5</sub> | 10,680   | 0.0676                          | 0.0677  | 0.0605   |
|                    | CNN <sub>6-5</sub> | 12,300   | 0.0695                          | 0.0691  | 0.0627   |
| CIFAR10            | 3x50               | 160      | 0.0045                          | 0.0046  | 0.0042   |
|                    | 5x100              | 510      | 0.0038                          | 0.0037  | 0.0033   |
|                    | CNN <sub>3-2</sub> | 3,378    | 0.0312                          | 0.0313  | 0.0311   |
|                    | CNN <sub>6-5</sub> | 17,110   | 0.0224                          | 0.0223  | 0.0212   |

tight upper bound because the enclosed area between it and the activation function is minimal. In Wu and Zhang’s approach, they adopted the tangent line that is parallel to the lower bound as its upper bound, as shown in Figure 3d. Some other approaches such as [5, 26, 55] adopt similar approximation strategies, but they have been experimentally proved not as tight as the ones in [18, 51].

Lyu et al. [28] proposed a gradient-based searching approach for computing a tighter approximation if the approximation can produce tighter input intervals for the following neurons. However, the experimental results in the work [51] show that this approach neither guarantees it always produces larger certified lower robust bound than other approaches and its scalability is rather limited due to the complexity of the searching algorithm for each neuron.

Table 1 shows the comparison results, where, surprisingly, none of these approaches surpass the others for all the networks. We also observe that VERINET won the competition on 13 out of 20 networks, while DEEPCERT on the remaining ones. This indicates that the performances of these so-called tight approaches vary case by case. In this paper we do not intend to judge which approach is better experimentally but focus on seeking theoretical foundations for the tightness of approximations. The comparison result showed that existing tightness definitions do not rigorously guarantee that

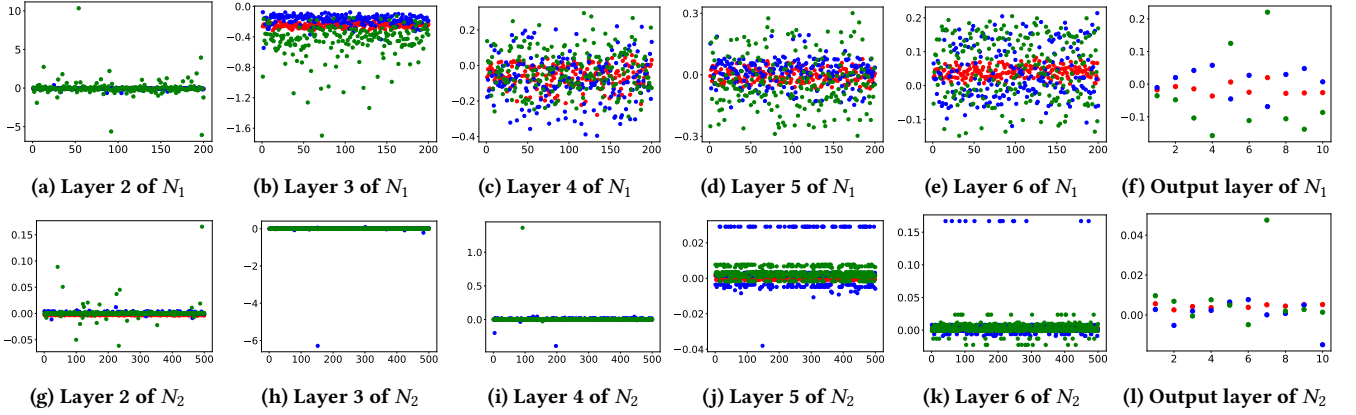


**Figure 4: Visualization of intermediate intervals during layer-by-layer propagation under different approximations (Red dot:  $\frac{(u-l)-(u'-l')}{u'-l'}$ ; blue dot:  $\frac{l-l'}{l'}$ ; green dot:  $\frac{u-u'}{u'}$ ;  $[l, u]$ : interval computed by VERINET,  $[l', u']$ : interval computed by DEEPCERT).**

a tighter approximation can always produce a larger robust bound. This motivates us to seek a unified definition to characterize the *tightness* of approximations for robustness verification of neural networks.

### 3.2 Empirical Analysis

To validate our observation on the tightness issue and investigate its generality, we have performed empirical analysis of three state-of-the-art approximation approaches, i.e., DEEPCERT [51], VERINET [18], and ROBUSTVERIFIER [26], on 20 sigmoid neural networks collected from the public benchmarks. We evaluate the tightness of these approaches by computing the lower robust bound for each network using the tools, respectively. We randomly selected 100 images for each network, computed their lower robust bounds, and took the average value. Computing averaged lower bounds is a widely-adopted approach to reduce the affect of floating-point errors [28, 47, 51]. Thus, even a small difference in the averaged value reflects a big difference in individual input. In general, the larger bound indicates the corresponding tool has a better performance.

We empirically analyzed the layer-by-layer propagation in the verification process of the best two tools VERINET and DEEPCERT and identified the missing factor that influences verification results. We tracked the computation of the intermediate intervals of the neurons on hidden layers during their layer-by-layer propagation and compared their tightness under different approximation strategies.

Figure 4 shows the layer-by-layer comparison of the intermediate intervals on the hidden neurons and output neurons. These intervals are computed during verification using the approximation approaches in [18, 51], respectively. The figures from Figure 4a to 4f show one 5-hidden-layer network named  $N_1$  on which VERINET computes a larger bound than DEEPCERT, while those from Figure 4g to 4l show another 5-hidden-layer network named  $N_2$  on which DEEPCERT computes a larger bound than VERINET. For each neuron, we use  $[l, u]$  and  $[l', u']$  to represent the intervals computed by VERINET and DEEPCERT, respectively. We introduce three dots in red, blue and green to represent  $\frac{(u-l)-(u'-l')}{u'-l'}$ ,  $\frac{l-l'}{l'}$  and  $\frac{u-u'}{u'}$ , respectively. The  $x$ -axis represents the neurons on the corresponding layer, and the  $y$ -axis represents the differences of the interval length, lower bounds, and upper bounds of the intervals.

Horizontally on  $N_1$ , most of the red dots are below 0 from layer 2 to the output layer, except layer 6. That indicates the intervals computed by VERINET usually have smaller (tighter) sizes than those by DEEPCERT. The blue dots gradually move up above 0, indicating that the lower bounds of the intervals computed by VERINET become greater than the those by DEEPCERT. Similarly, the green dots gradually move down below 0, indicating that the upper bounds computed by VERINET become smaller. The trends of the three values reflect that the intermediate intervals computed by VERINET are statistically tighter than those by DEEPCERT on network  $N_1$ .

The trend of intermediate intervals on network  $N_2$  is an opposite of the one on  $N_1$ . The red dots move up above 0 layer by layer, indicating that the interval sizes computed by VERINET become larger than those by DEEPCERT. The blue dots gradually move down below 0 and the green ones move up above 0.

The analysis result from Figure 4 reveals that the intermediate intervals are statistically tighter than other tools when a tool produces larger certified lower bounds.

### 3.3 The Network-Wise Tightest Approximation

Existing characterizations of tightness are individually heuristic under a presumption that a tighter approximation gives rise to a more precise verification result. Unfortunately, the above examples show that this presumption does not always hold. It means that defining the tightness on each individual neuron is neither sufficient nor necessary for achieving tight approximations. That is because the tightness on neurons cannot guarantee the output intervals of neural networks are always precise. However, the output intervals are the basis for judging whether a network is robust or not.

To characterize the tightness of approximations to the activation functions in a neural network, we introduce the notion of *network-wise tightness*. We ensure that, by a network-wise tighter approximation of the activation functions, the approximated neural network must produce more precise output intervals and consequently more precise verification results.

**DEFINITION 3 (NETWORK-WISE TIGHTNESS).** *Given a neural network  $f : \mathbb{R}^n \rightarrow \mathbb{R}^m$  and  $x \in \mathbb{B}_p(x_0, \epsilon)$ , let  $(f_L, f_U)$  be a linear*

approximation of  $f$  with  $f_U$  and  $f_L$  the upper and lower bounds, respectively.  $(f_L, f_U)$  is network-wise tightest if, for any different linear approximation  $(\hat{f}_L, \hat{f}_U)$ ,

$$\forall s \in S, \quad \min_{x \in \mathbb{B}_p(x_0, \epsilon)} f_{L,s}(x) \geq \min_{x \in \mathbb{B}_p(x_0, \epsilon)} \hat{f}_{L,s}(x),$$

$$\max_{x \in \mathbb{B}_p(x_0, \epsilon)} f_{U,s}(x) \leq \max_{x \in \mathbb{B}_p(x_0, \epsilon)} \hat{f}_{U,s}(x),$$

where  $f_{L,s}(x)$ ,  $f_{U,s}(x)$  denote  $s$ -th item of  $f_L(x)$ ,  $f_U(x)$ , respectively.

Intuitively,  $(f_L, f_U)$  is tighter than  $(\hat{f}_L, \hat{f}_U)$  in that for all output neurons  $s$ ,  $f_L$  (resp.  $f_U$ ) always computes a lower (resp. an upper) bound that is greater (resp. less) than the one  $\hat{f}_L$  (resp.  $\hat{f}_U$ ) does. Note that Definition 3 is universal in that it is applicable to (i) all activation functions and (ii) all  $\ell_p$  norms.

**Example 3.** By Definition 3, the approximations  $x_{U,3}$ ,  $x_{L,3}$ ,  $x_{U,4}$ ,  $x_{L,4}$  to the activation functions on  $x_3$  and  $x_4$  in Example 2 are tighter than  $x'_{U,3}$ ,  $x'_{L,3}$ ,  $x'_{U,4}$ ,  $x'_{L,4}$ . This is consistent to the verification results. Using the former approximations, we can compute tighter output ranges for both  $x_5$  and  $x_6$  than those by the latter. However, the former approximation can be proved to be less tight than the latter if we take the tightness definition with respect to the minimal area defined in [18].

Next, we give an important property of the network-wise tightness. That is, a network-wise tighter approximation always leads to more precise verification results.

**THEOREM 1.** *The approximation  $(f_L, f_U)$  of a neural network always produces more precise robustness verification result than  $(\hat{f}_L, \hat{f}_U)$  if  $(f_L, f_U)$  is tighter than  $(\hat{f}_L, \hat{f}_U)$  by Definition 3.*

**PROOF SKETCH.** Let  $s_0 = \mathcal{L}(f(x_0))$  with fixed  $\epsilon$ . We check for all  $s$  other than  $s_0$  whether the following condition:

$$\min_{x \in \mathbb{B}_p(x_0, \epsilon)} f_{L,s_0}(x) > \max_{x \in \mathbb{B}_p(x_0, \epsilon)} f_{U,s}(x) \quad (8)$$

holds. By Definition 3, if  $(\hat{f}_L, \hat{f}_U)$  satisfies (8), then we have:

$$\min_{x \in \mathbb{B}_p(x_0, \epsilon)} \hat{f}_{L,s_0}(x) \geq \min_{x \in \mathbb{B}_p(x_0, \epsilon)} \hat{f}_{L,s_0}(x) >$$

$$\max_{x \in \mathbb{B}_p(x_0, \epsilon)} \hat{f}_{U,s}(x) \geq \max_{x \in \mathbb{B}_p(x_0, \epsilon)} f_{U,s}(x),$$

for all  $s$  other than  $s_0$ . Thus,  $(f_L, f_U)$  certainly satisfies (8) as well. Namely, the result verified by  $(\hat{f}_L, \hat{f}_U)$  can also be deduced by  $(f_L, f_U)$ . On the contrary, the result verified by  $(f_L, f_U)$  may not be verified by  $(\hat{f}_L, \hat{f}_U)$ . Consequently,  $(f_L, f_U)$  always produce more precise verification result than  $(\hat{f}_L, \hat{f}_U)$ .  $\square$

Next, we show that computing the network-wise tightest approximation is essentially an optimization problem. Given a  $k$ -layer neural network  $f: \mathbb{R}^n \rightarrow \mathbb{R}^m$ , we use  $\phi^t$  to denote the compound function of  $f$ 's layers before  $t$ -th activation function is applied, i.e.,

$$\phi^t = f^t \circ \sigma^{t-1} \circ f^{t-1} \circ \dots \circ \sigma^1 \circ f^1.$$

For layer  $t$  with  $n^t$  neurons, let  $\phi_r^t(x)$  indicate  $r$ -th item of its output (with  $r \in \mathbb{Z}$  and  $1 \leq r \leq n^t$ ). For each activation function  $\sigma(x)$  with  $x \in [l, u]$ , we denote the upper (resp. lower) bound of  $\sigma(x)$  by  $h_U(x) = \alpha_U x + \beta_U$  (resp.  $h_L(x) = \alpha_L x + \beta_L$ ), with variables  $\alpha_L, \alpha_U, \beta_L, \beta_U \in \mathbb{R}$ . The problem of computing the network-wise

tightest approximation can then be formalized as the following optimization problems:

$$\max(\min_{x \in \mathbb{B}_\infty(x_0, \epsilon)} (A_{L,s}^k x + B_{L,s}^k)), \text{ and} \quad (9)$$

$$\min(\max_{x \in \mathbb{B}_\infty(x_0, \epsilon)} (A_{U,s}^k x + B_{U,s}^k)) \quad (10)$$

$$\text{s.t. } \forall r \in \mathbb{Z}, 1 \leq r \leq n^t, \forall t \in \mathbb{Z}, 1 \leq t < k,$$

$$\begin{cases} \alpha_{L,r}^t z_r^t + \beta_{L,r}^t \leq \sigma(z_r^t) \leq \alpha_{U,r}^t z_r^t + \beta_{U,r}^t; \\ \min_{x \in \mathbb{B}_\infty(x_0, \epsilon)} A_{L,r}^t x + B_{L,r}^t \leq z_r^t \leq \max_{x \in \mathbb{B}_\infty(x_0, \epsilon)} A_{U,r}^t x + B_{U,r}^t. \end{cases}$$

Here,  $A_{L,r}^t x + B_{L,r}^t$  and  $A_{U,r}^t x + B_{U,r}^t$  are the lower and upper linear bounds of  $\phi_r^t(x)$ , respectively.  $A_{L,r}^t, A_{U,r}^t, B_{L,r}^t$  and  $B_{U,r}^t$  are constant tensors defined on  $W^t, b^t$ , where  $W^t, b^t$  are the weights and biases of the  $t$ -th layer.  $\phi_r^t$  is the compound function of  $f$ 's first  $t$  layers.  $\phi_r^t(x)$  can be approximated by a lower linear bound  $A_{L,r}^t x + B_{L,r}^t$  and an upper linear bound  $A_{U,r}^t x + B_{U,r}^t$  with:

$$A_{L,r}^t = \begin{cases} W_r^t, & t = 1 \\ W_{\geq 0,r}^t \alpha_{L,r}^{t-1} \odot A_{L,r}^{t-1} + W_{< 0,r}^t \alpha_{U,r}^{t-1} \odot A_{L,r}^{t-1}, & t \geq 2 \end{cases}$$

$$B_{L,r}^t = \begin{cases} b_r^t, & t = 1 \\ W_{\geq 0,r}^t (\alpha_{L,r}^{t-1} \odot B_{L,r}^{t-1} + \beta_{L,r}^{t-1}) + \\ W_{< 0,r}^t (\alpha_{U,r}^{t-1} \odot B_{L,r}^{t-1} + \beta_{L,r}^{t-1}) + b_r^t, & t \geq 2 \end{cases}$$

$$A_{U,r}^t = \begin{cases} W_r^t, & t = 1 \\ W_{\geq 0,r}^t \alpha_{U,r}^{t-1} \odot A_{U,r}^{t-1} + W_{< 0,r}^t \alpha_{L,r}^{t-1} \odot A_{U,r}^{t-1}, & t \geq 2 \end{cases}$$

$$B_{U,r}^t = \begin{cases} b_r^t, & t = 1 \\ W_{\geq 0,r}^t (\alpha_{U,r}^{t-1} \odot B_{U,r}^{t-1} + \beta_{U,r}^{t-1}) + \\ W_{< 0,r}^t (\alpha_{L,r}^{t-1} \odot B_{U,r}^{t-1} + \beta_{U,r}^{t-1}) + b_r^t, & t \geq 2 \end{cases}$$

where  $\odot$  denotes Hadamard production.

The solutions to all  $\alpha_L, \alpha_U, \beta_L, \beta_U$  are the linear bounds to all the activation functions in the network, and their composition is the network-wise tightest approximation. Note that the solutions may not guarantee that the approximation to an individual activation function is the tightest with respect to existing tightness definitions.

## 4 APPROACH FOR 1-HIDDEN-LAYER NETWORKS

Given a neural network, we can compute the network-wise tightest approximation by instantiating and solving the optimization problems (9) and (10). For a one-hidden-layer network, the optimization problems can be simplified as follows:

$$\max(\min_{x \in \mathbb{B}_\infty(x_0, \epsilon)} (A_{L,s} x + B_{L,s})), \quad (11)$$

$$\min(\max_{x \in \mathbb{B}_\infty(x_0, \epsilon)} (A_{U,s} x + B_{U,s})), \quad (12)$$

$$\text{s.t. } \forall r \in \mathbb{Z}, 1 \leq r \leq n,$$

$$\begin{cases} \alpha_{L,r} z_r + \beta_{L,r} \leq \sigma(z_r) \leq \alpha_{U,r} z_r + \beta_{U,r}; \\ \min_{x \in \mathbb{B}_\infty(x_0, \epsilon)} W^1 x + b^1 \leq z_r \leq \max_{x \in \mathbb{B}_\infty(x_0, \epsilon)} W^1 x + b^1. \end{cases}$$

where  $A_{L,s} = W_{\geq 0,s}^2 (\alpha_L \odot W^1) + W_{< 0,s}^2 (\alpha_U \odot W^1)$ ,  $B_{L,s} = W_{\geq 0,s}^2 (\alpha_L \odot b^1 + \beta_L) + W_{< 0,s}^2 (\alpha_U \odot b^1 + \beta_U) + b_s^2$ ,  $n$  denotes the amount of neurons in the hidden layer. The above optimization problems are the instances of the problems (9) and (10).

**Algorithm 1:** A gradient descent-based searching algorithm for the tightest approximations of 1-hidden-layer networks.

**Input** :  $N$ : a network;  $x_0$ : an input to  $N$ ;  $\epsilon$ : a  $\ell_\infty$ -norm radius

**Output**:  $\alpha_{L,r}, \beta_{L,r}, \alpha_{U,r}, \beta_{U,r}$  for each hidden neuron  $r$

```

1 for each neuron  $r$  do
2   Evaluate input range  $[l_r, u_r]$  for  $r$ ;
3   Let  $\omega$  denote the line connecting  $(l_r, \sigma(l_r))$  and  $(u_r, \sigma(u_r))$ ;
4    $R_L \leftarrow \emptyset, R_U \leftarrow \emptyset$ ; // Empty the sets of optimizable neurons.
5   if  $\omega$  can be an upper bound of  $\sigma$  then
6     Let  $\alpha_{U,r}, \beta_{U,r}$  be the slope and intercept of  $\omega$ ;
7     Add  $(r, [l_r, u_r])$  to  $R_L$ ; //  $r$ 's lower bound is optimizable.
8   else if  $\omega$  can be a lower bound of  $\sigma$  then
9     Let  $\alpha_{L,r}, \beta_{L,r}$  be the slope and intercept of  $\omega$ ;
10    Add  $(r, [l_r, u_r])$  to  $R_U$ ; //  $r$ 's upper bound is optimizable.
11  else
12    Let  $z_{U,r}, z_{L,r}$  be the cut-off points of the tangent lines
13    of  $\sigma$  crossing  $(l_r, \sigma(l_r))$  and  $(u_r, \sigma(u_r))$ ;
14    Add  $(r, [z_{U,r}, u_r])$  to  $R_U$ , and  $(r, [l_r, z_{L,r}])$  to  $R_L$ ;
15  Randomize the cut-off points for optimizable bounds of  $r$ ;
16  Let  $\alpha_{L,r}, \beta_{L,r}, \alpha_{U,r}, \beta_{U,r}$  be the slope and intercept of
17  tangent line of  $\sigma$  at chosen cut-off points;
18 for  $1, \dots, k$  do //  $k$  is the preset optimization round
19  Compute  $A_{L,s}, B_{L,s}$  of the lower bound of output neuron  $s$ ;
20  Let  $G := \min_{x \in \mathbb{B}_\infty(x_0, \epsilon)} (A_{L,s}x + B_{L,s})$ ;
21  Update the cut-off points for  $r$ 's bound through  $-\nabla(G)$ ;
22  Update  $\alpha_{L,r}, \beta_{L,r}, \alpha_{U,r}, \beta_{U,r}$  at chosen cut-off points;

```

The optimization problem is a convex variant and thus efficiently solvable by leveraging the gradient descent-based searching algorithm [28]. Algorithm 1 shows the pseudo code of the algorithm for calculating the optimal solution for the optimization problem with objective function (11). A solution represents a network-wise tightest lower bound to the 1-hidden-layer networks. For each activation function on a hidden neuron, it first determines whether the line  $\omega$  crossing the two endpoints can be an upper (Lines 5-7) or lower bound (Lines 8-10). If those are the cases, the tangent line of the activation function is chosen to be lower bound (*resp.* upper bound), and its cut-off point can be an optimization variable. Otherwise (Lines 11-13), the lower and upper bounds can both be optimized. The optimizing ranges for those cases are calculated.

Let  $G := \min_{x \in \mathbb{B}_\infty(x_0, \epsilon)} (A_{L,s}x + B_{L,s})$  and  $ANS = \max_{\alpha_L, \alpha_U, \beta_L, \beta_U} (G)$ . We use gradient descent steps (Lines 16-20) to optimize the target ANS. We conduct gradient descent and modify the value of  $\alpha_L, \alpha_U, \beta_L, \beta_U$  if the ANS achieves a larger result under the new bounds.

The optimization problem with objective function (12) can be solved by the same algorithm, with ANS replaced by (12).

**Example 4.** Let us revisit Example 2. With Algorithm 1, we compute the network-wise tightest approximations for the network in Figure 2. Figure 5 shows the upper (*resp.* lower) bounds, denoted by  $x''_{U,3}, x''_{U,4}$  (*resp.*  $x''_{L,3}, x''_{L,4}$ ). By Definition 3,  $x''_{U,3}, x''_{U,4}$  are tighter than the other two approximations. The resulting output range of neuron  $x_7$  is  $[0.307, 5.693]$ , which is more precise than both  $[-0.079, 6.073]$  and  $[0.177, 5.817]$  in Figure 3a and 3b, respectively.

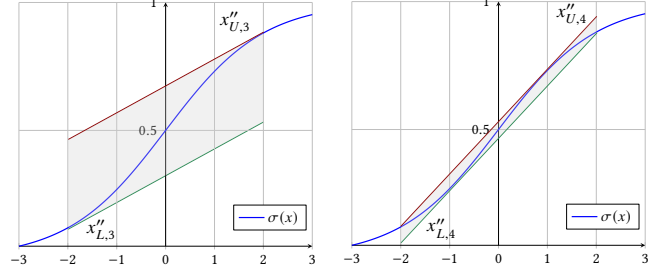


**Figure 5:** The network-wise tightest approximation to the activation functions on  $x_3$  (left) and  $x_4$  (right) in Example 2.

Note that the network-wise tightest approximations in the above example are a hybrid of both kinds of approximations in Figure 3a and 3b, which cannot be the tightest under a single tightness criterion in [18, 51]. This echoes our advocacy that solely pursuing neuron-wise tightness under existing tightness definitions may not guarantee that they are the network-wise tightest, and consequently cannot achieve precise robust verification results.

## 5 APPROACH FOR MULTI-HIDDEN-LAYER NETWORKS

For the networks with two or more hidden layers, solving the optimization problems (9) and (10) becomes impractical due to its non-convexity. In [28], Lyu *et al.* proved that it is even non-convex to separately compute the tightest approximation for each neuron. The intractability lies in the accumulated constraints throughout the network: for any hidden layer, the input intervals of the activation functions are constrained by the approximations to the activation functions for the previous hidden layer. Neither can the optimization problems be solved on a layer basis because the objective function are network-wise. To our knowledge, no efficient algorithms or tools exist for such optimization problems. In this section, we propose computable neuron-wise tightest approximations and identify the condition when all the weights in a neural network are non-negative, the neuron-wise tightest approximations lead to being network-wise tightest.

### 5.1 The Neuron-Wise Tightest Approximation

Our empirical analysis in Section 3.1 reveals an insight that preserving tighter intermediate intervals during layer-by-layer propagation usually produces larger certified lower robust bounds. In the same spirit, we heuristically define the tightness of an approximation to an individual activation function in terms of the overestimation caused by the approximation. Smaller overestimation implies a tighter approximation. Particularly, an approximation is the *neuron-wise tightest* if it results in no overestimation of the output range of the activation function.

**DEFINITION 4 (NEURON-WISE TIGHTNESS).** Let  $\sigma(x)$  be an activation function with  $x \in [l, u]$ , and  $h_U(x), h_L(x)$  be its upper and lower bounds, with  $\alpha_U, \alpha_L$  their slopes.  $h_U(x)$  (*resp.*  $h_L(x)$ ) is the neuron-wise tightest if  $h_U(u) = \sigma(u)$  (*resp.*  $h_L(l) = \sigma(l)$ ) and  $\int_l^u h_U(x) - \sigma(x) dx$  (*resp.*  $\int_l^u \sigma(x) - h_L(x) dx$ ) is minimal.

By Definition 4, we identify three cases of defining the neuron-wise tightest approximation for each individual activation function. The three cases are defined according to the relation between the slopes of activation function at two endpoints and the slope of

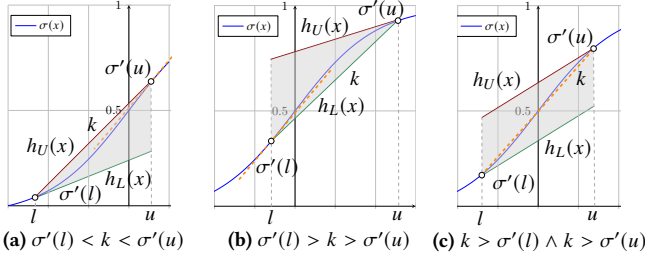


Figure 6: The neuron-wise tightest linear approximation.

the line crossing the two endpoints, as classified in [18, 51]. Given an input interval  $[l, u]$  for  $\sigma(x)$ , the slopes of  $\sigma(x)$  at  $(l, \sigma(l))$  and  $(u, \sigma(u))$  are represented by  $\sigma'(l)$  and  $\sigma'(u)$ , respectively; the slope of the line crossing  $(l, \sigma(l))$  and  $(u, \sigma(u))$  is  $k = \frac{\sigma(u) - \sigma(l)}{u - l}$ . Figure 6 depicts the neuron-wise tightest approximations in the following three different cases:

**Case 1.** When  $\sigma'(l) < k < \sigma'(u)$  (Figure 6a), the line that connects the two endpoints is chosen as the upper bound, while the tangent line of  $\sigma(x)$  at  $(l, \sigma(l))$  as the lower bound. We then have  $h_U(x) = k(x - l) + \sigma(l)$  and  $h_L(x) = \sigma'(l)(x - l) + \sigma(l)$ .

**Case 2.** When  $\sigma'(u) < k < \sigma'(l)$  (Figure 6b), the tangent line of  $\sigma(x)$  at  $(u, \sigma(u))$  and the line crossing two endpoints are considered as the upper and lower bounds, respectively. We then have  $h_U(x) = \sigma'(u)(x - u) + \sigma(u)$  and  $h_L(x) = k(x - u) + \sigma(u)$ .

**Case 3.** When  $\sigma'(l) < k$  and  $\sigma'(u) < k$  (Figure 6c), the tangent line of  $\sigma(x)$  at  $(u, \sigma(u))$  is taken as the upper bound, while the tangent line of  $\sigma(x)$  at  $(l, \sigma(l))$  as the lower bound. We then have  $h_U(x) = \sigma'(u)(x - u) + \sigma(u)$  and  $h_L(x) = \sigma'(l)(x - l) + \sigma(l)$ .

Note that, Definition 4 also considers the tightness characterizations in [18, 28]. It is easy to prove that any other linear bound crossing the endpoints is less tight than the one defined in the above three cases according to the tightness definitions in [18, 28].

## 5.2 Neuron-Wise vs. Network-Wise

In this section, we study the relation between neuron-wise tightness and network-wise tightness. Although the neuron-wise tightest approximation does not overestimate the output range of a single neuron, it cannot guarantee that the composition for all the neurons is the network-wise tightest because the monotonicity of a neuron cannot be preserved by the next layer. The monotonicity may be altered by the weights between layers because the input function of each neuron in any hidden layer is compounded by the output functions in the previous layer multiplied by the weights. Hence, a sufficient condition of passing neuron-wise tightness to the network is to avoid breaking monotonicity during the propagation.

**DEFINITION 5 (NETWORK-WISE MONOTONOUS).** Given a  $k$ -layer neural network  $f : \mathbb{R}^n \rightarrow \mathbb{R}^m$  and its input  $x = [x_1, \dots, x_n]$ ,  $f$  is called network-wise monotonus if the following three conditions hold:

- (1)  $\forall t_1, t_2 \in \mathbb{Z}, 1 \leq t_1 \leq k \wedge 1 \leq t_2 \leq k$ ,
- (2)  $\forall r_1, r_2 \in \mathbb{Z}, 1 \leq r_1 \leq n^{t_1} \wedge 1 \leq r_2 \leq n^{t_2}$ ,
- (3)  $\forall i \in \mathbb{Z}, 1 \leq i \leq n, \phi_{r_1}^{t_1}(x_i), \phi_{r_2}^{t_2}(x_i)$  are both either monotonically increasing or decreasing.

Intuitively, a monotonous network requires all the neurons to share the same monotonicity w.r.t. the input so that they can achieve the maximum or minimum on the same input.

**LEMMA 1.** A neural network is network-wise monotonous if the network satisfies the following two conditions:

- (1) For the first layer, for any selected  $i \in \mathbb{Z}, 1 \leq i \leq n$ , items in the  $i$ -th column of  $W^1$  are all positive or all negative;
- (2) Every item in weights from the second layer to the last layer is non-negative.

Next, we formulate the most important property of our neuron-wise approximation approach as the following theorem, stating that the composition of all neuron-wise tightest approximations is the network-wise tightest if the network is monotonous.

**THEOREM 2.** The composition of the neuron-wise tightest approximations is the network-wise tightest if the network satisfies the following two conditions:

- (1) For the first layer, the items in each column of the weight matrix are all positive or negative;
- (2) Every item in weights between remained layers is non-negative.

Theorem 2 holds as both conditions guarantee the monotonicity of the network. If a neural network is monotonous, then the composition of the neuron-wise tightest approximations is a network-wise tightest approximation with respect to the robustness verification. In particular, starting from the second layer, the neuron-wise tightness is preserved with only non-negative weights during the layer-wise propagation (the second condition). See [56, Appendix B] for the complete proof.

**Example 5.** Assume that we replace the three negative weights of the neural network in Figure 2 with 1, 5, and 1, respectively. The tightest approximations to  $x_3$  and  $x_4$ , returned by Algorithm 1, are exactly the same as those returned by the neuron-wise tightest approximations in Section 5.1 (i.e.,  $[1.430, 10.570]$ ).

## 6 EXPERIMENTS

We evaluate our approximation method concerning both precision and efficiency in the robustness verification of Sigmoid-like neural networks. Our goal is threefold:

- (1) To validate our mathematical proof of Theorem 2 via extensive experimental results (i.e., always returning the largest certified lower bounds for non-negative networks);
- (2) To demonstrate that Algorithm 1 can always compute tighter lower bounds for 1-hidden-layer networks;
- (3) To explore our approach's effectiveness under general neural networks with *mixed* weights.

### 6.1 Benchmarks and Experimental Setup

**Competitors.** We consider three representative approximations in the literature: DEEPCERT [51], VERINET [18], and ROBUSTVERIFIER [26]. For a fair comparison, we implemented in Python all the competing approaches including our new algorithm called NEWISE.

**Datasets and Networks.** We have conducted three sets of experiments on fully connected (FNNs) and convolutional (CNNs) networks: We focus on CNNs due to their effectiveness in a wide



**Table 2: Performance comparison on non-negative Sigmoid networks between NEWISE (NW) and existing tools, DEEPCERT (DC), VERINET (VN), and ROBUSTVERIFIER (RV).  $t \times n$  refers to an FNN with  $t$  layers and  $n$  neurons per layer.  $\text{CNN}_{t-c}$  denotes a CNN with  $t$  layers and  $c$  filters of size  $3 \times 3$ .**

| Dataset            | Model              | #Neur. | Certified Lower Bound |        |           |        |           |        |                    |        |        |           |         |           | Time (s) |            |              |
|--------------------|--------------------|--------|-----------------------|--------|-----------|--------|-----------|--------|--------------------|--------|--------|-----------|---------|-----------|----------|------------|--------------|
|                    |                    |        | Average               |        |           |        |           |        | Standard Deviation |        |        |           |         |           |          |            |              |
|                    |                    |        | NW                    | DC     | Impr. (%) | VN     | Impr. (%) | RV     | Impr. (%)          | NW     | DC     | Impr. (%) | VN      | Impr. (%) |          | RV         | Impr. (%)    |
| MNIST              | 5x100              | 510    | 0.0091                | 0.0071 | 28.15 ↑   | 0.0071 | 27.25 ↑   | 0.0064 | 40.90 ↑            | 0.0057 | 0.0042 | 37.11 ↑   | 0.0042  | 35.48 ↑   | 0.0034   | 69.35 ↑    | 4.30 ±0.02   |
|                    | 3x700              | 2,110  | 0.0037                | 0.0030 | 24.92 ↑   | 0.0030 | 22.85 ↑   | 0.0029 | 27.05 ↑            | 0.0018 | 0.0013 | 41.86 ↑   | 0.0014  | 34.56 ↑   | 0.0013   | 41.86 ↑    | 117.94 ±0.31 |
|                    | CNN <sub>6-5</sub> | 12,300 | 0.0968                | 0.0788 | 22.82 ↑   | 0.0778 | 24.37 ↑   | 0.0699 | 38.50 ↑            | 0.0372 | 0.0280 | 32.92 ↑   | 0.0276  | 35.09 ↑   | 0.0212   | 75.86 ↑    | 5.70 ±0.42   |
|                    | 3x50               | 160    | 0.0105                | 0.0088 | 19.23 ↑   | 0.0088 | 19.50 ↑   | 0.0080 | 31.42 ↑            | 0.0051 | 0.0038 | 32.72 ↑   | 0.0038  | 32.72 ↑   | 0.0029   | 71.86 ↑    | 0.14 ±0.00   |
|                    | 3x100              | 310    | 0.0139                | 0.0120 | 15.46 ↑   | 0.0120 | 15.56 ↑   | 0.0111 | 25.47 ↑            | 0.0071 | 0.0057 | 24.82 ↑   | 0.0057  | 23.30 ↑   | 0.0046   | 53.46 ↑    | 2.22 ±0.02   |
|                    | CNN <sub>5-5</sub> | 10,680 | 0.0801                | 0.0708 | 13.14 ↑   | 0.0704 | 13.75 ↑   | 0.0683 | 17.30 ↑            | 0.0238 | 0.0200 | 18.87 ↑   | 0.0198  | 20.50 ↑   | 0.0180   | 32.20 ↑    | 2.88 ±0.32   |
|                    | CNN <sub>3-2</sub> | 2,514  | 0.0521                | 0.0483 | 7.82 ↑    | 0.0483 | 7.94 ↑    | 0.0478 | 8.88 ↑             | 0.0180 | 0.0161 | 12.13 ↑   | 0.0160  | 12.41 ↑   | 0.0156   | 15.44 ↑    | 0.17 ±0.04   |
|                    | CNN <sub>4-5</sub> | 8,680  | 0.0505                | 0.0473 | 6.68 ↑    | 0.0471 | 7.26 ↑    | 0.0464 | 8.81 ↑             | 0.0207 | 0.0186 | 11.26 ↑   | 0.0183  | 12.84 ↑   | 0.0175   | 17.87 ↑    | 1.17 ±0.20   |
| CNN <sub>3-4</sub> | 5,018              | 0.0448 | 0.0422                | 6.09 ↑ | 0.0421    | 6.24 ↑ | 0.0418    | 6.98 ↑ | 0.0156             | 0.0142 | 9.71 ↑ | 0.0141    | 10.18 ↑ | 0.0138    | 12.56 ↑  | 0.30 ±0.08 |              |
| Fashion MNIST      | 4x100              | 410    | 0.0312                | 0.0188 | 65.48 ↑   | 0.0194 | 60.62 ↑   | 0.0159 | 96.22 ↑            | 0.0403 | 0.0210 | 92.28 ↑   | 0.0220  | 83.20 ↑   | 0.0176   | 129.47 ↑   | 3.31 ±0.04   |
|                    | 3x100              | 310    | 0.0326                | 0.0263 | 24.02 ↑   | 0.0270 | 21.03 ↑   | 0.0238 | 36.81 ↑            | 0.0335 | 0.0262 | 27.67 ↑   | 0.0282  | 18.92 ↑   | 0.0234   | 43.22 ↑    | 2.22 ±0.01   |
|                    | CNN <sub>5-5</sub> | 10,680 | 0.1303                | 0.1155 | 12.81 ↑   | 0.1151 | 13.22 ↑   | 0.1088 | 19.72 ↑            | 0.0830 | 0.0714 | 16.23 ↑   | 0.0721  | 15.10 ↑   | 0.0636   | 30.51 ↑    | 2.89 ±0.33   |
|                    | CNN <sub>3-2</sub> | 2,514  | 0.0790                | 0.0713 | 10.79 ↑   | 0.0713 | 10.74 ↑   | 0.0695 | 13.68 ↑            | 0.0497 | 0.0416 | 19.55 ↑   | 0.0418  | 19.06 ↑   | 0.0386   | 28.98 ↑    | 0.17 ±0.04   |
|                    | CNN <sub>4-5</sub> | 8,680  | 0.0959                | 0.0868 | 10.40 ↑   | 0.0864 | 10.90 ↑   | 0.0839 | 14.19 ↑            | 0.0561 | 0.0486 | 15.51 ↑   | 0.0482  | 16.52 ↑   | 0.0453   | 24.03 ↑    | 1.18 ±0.21   |
|                    | CNN <sub>3-4</sub> | 5,018  | 0.0747                | 0.0694 | 7.52 ↑    | 0.0693 | 7.72 ↑    | 0.0681 | 9.70 ↑             | 0.0465 | 0.0410 | 13.32 ↑   | 0.0409  | 13.59 ↑   | 0.0391   | 18.85 ↑    | 0.30 ±0.09   |
| CIFAR10            | 9x100              | 910    | 0.0315                | 0.0211 | 49.03 ↑   | 0.0214 | 46.94 ↑   | 0.0192 | 63.58 ↑            | 0.0280 | 0.0183 | 52.70 ↑   | 0.0186  | 50.32 ↑   | 0.0133   | 110.07 ↑   | 4.92 ±0.01   |
|                    | 6x100              | 610    | 0.0221                | 0.0174 | 27.08 ↑   | 0.0176 | 26.14 ↑   | 0.0170 | 30.22 ↑            | 0.0165 | 0.0118 | 40.05 ↑   | 0.0120  | 37.82 ↑   | 0.0111   | 48.24 ↑    | 3.04 ±0.02   |
|                    | 5x100              | 510    | 0.0200                | 0.0167 | 19.76 ↑   | 0.0167 | 19.47 ↑   | 0.0163 | 22.40 ↑            | 0.0137 | 0.0104 | 31.80 ↑   | 0.0104  | 31.42 ↑   | 0.0099   | 38.45 ↑    | 2.44 ±0.01   |
|                    | 3x50               | 160    | 0.0206                | 0.0178 | 15.43 ↑   | 0.0179 | 14.66 ↑   | 0.0176 | 16.88 ↑            | 0.0144 | 0.0113 | 27.57 ↑   | 0.0115  | 25.24 ↑   | 0.0110   | 31.30 ↑    | 0.43 ±0.00   |
|                    | 4x100              | 410    | 0.0161                | 0.0140 | 15.23 ↑   | 0.0140 | 14.81 ↑   | 0.0138 | 16.56 ↑            | 0.0111 | 0.0089 | 24.61 ↑   | 0.0090  | 23.63 ↑   | 0.0087   | 27.62 ↑    | 1.85 ±0.01   |
|                    | CNN <sub>3-4</sub> | 6,746  | 0.0187                | 0.0181 | 3.38 ↑    | 0.0181 | 3.32 ↑    | 0.0181 | 3.43 ↑             | 0.0109 | 0.0103 | 5.93 ↑    | 0.0103  | 5.83 ↑    | 0.0103   | 6.13 ↑     | 0.56 ±0.08   |
|                    | CNN <sub>3-2</sub> | 3,378  | 0.0185                | 0.0180 | 2.49 ↑    | 0.0180 | 2.55 ↑    | 0.0180 | 2.67 ↑             | 0.0125 | 0.0120 | 4.34 ↑    | 0.0120  | 4.34 ↑    | 0.0120   | 4.60 ↑     | 0.30 ±0.06   |

range of visual recognition applications [22, 27, 30, 34, 43]; we also consider FNNs to expand the architecture variety. We trained all the networks on the image databases MNIST [23], Fashion MNIST [53], and CIFAR10 [21]. We chose the first 100 images from the test set of each dataset as in [5, 51, 55], among which only correctly-classified images by the neural network are considered in our experiments.

For each network architecture, we trained three variant neural networks using the Sigmoid, Tanh, and Arctan activation functions, respectively. In Experiment I the networks contain only non-negative weights. We used Adam or SGD optimizer with at least 50 epochs of batch size 128. The test set accuracy of networks trained on MNIST, Fashion MNIST, and CIFAR10 is around 0.9, 0.85, and 0.4, respectively. In Experiment II and III we trained 1-hidden-layer networks and used pre-trained models [2, 40, 51] (as in Table 1, Section 3.2) with no constraint on the weights. Note that the number of neurons in FNNs can be considerably fewer than that in CNNs [24], while the networks can still achieve up to 0.99 test accuracy.

**Metrics.** We use certified lower bound to assess *effectiveness*, and  $(\epsilon' - \epsilon)/\epsilon$  to quantify the precision improvement, where  $\epsilon'$  and  $\epsilon$  denote the lower bounds certified by NEWISE and each competing approach, respectively. We consider both *average* and *standard deviation* (SD) of certified lower bounds; in particular, SD is a suitable measure of sensitivity of the approximations to input images: A larger SD implies a better sensitivity [51]. For *efficiency*, we record the average computation time over the (correctly-classified) images. **Experimental Setup.** All the experiments were conducted on a workstation running Ubuntu 18.04 with a 2.35GHz 32-core AMD EPYC 7452 CPU and 128 GB memory.

## 6.2 Experimental Results

**Experiment I.** Table 2 shows the comparison results for 22 Sigmoid models with non-negative weights. Regarding the precision of verification results, our NEWISE computes significantly larger certified lower bounds than the competitors for *all* the models. In particular, for *average*, NEWISE achieves up to 96.22% improvement, i.e., FNNs with 4 hidden layers trained on Fashion MNIST. NEWISE improves the precision even more with *standard deviation* (up to 129.33%). This indicates that our approach is more sensitive to input images compared to the other approaches: The more the certified lower bound is improved, the larger deviation the network exhibits.

Regarding efficiency, all the approaches incur similar overhead as expected (they share the same complexity, i.e.,  $O(1)$  on each neuron). We use  $p \pm q$  to denote their average time cost  $p$  and the size of the interval  $2q$ . Table 3 presents the results on the Tanh models. NEWISE computes *even larger* certified lower bounds, e.g., with up to 251.28%. We omit the similar time overheads in Table 3. See [56, Appendix C] for the complete results, including those on the Arctan models.

All these experimental results provide strong independent validation of our mathematical proof of Theorem 2.

**Experiment II.** We evaluate the performance of Algorithm 1 on 1-hidden-layer networks. Table 4 shows the comparison results with the other three tools. We only show the metric of standard deviation due to space limit. As shown in the table, Algorithm 1 can compute larger bounds with up to 160.66% improvement. Complete results are available in the [56, Appendix C].

Regarding efficiency, the searching algorithm needs more time because it is in polynomial time, unlike the constant-time approach

**Table 3: Performance comparison of NEWISE (NW) with DEEPCERT (DC), VERINET (VN), and ROBUSTVERIFIER (RV) on non-negative Tanh networks.  $t \times n$  refers to an FNN with  $t$  layers and  $n$  neurons per layer.  $\text{CNN}_{t-c}$  denotes a CNN with  $t$  layers and  $c$  filters of size  $3 \times 3$ .**

| Dataset       | Model              | Certified Lower Bound (Standard Deviation) |        |           |        |           |        |           |
|---------------|--------------------|--|--------|-----------|--------|-----------|--------|-----------|
|               |                    | NW   | DC     | Impr. (%) | VN     | Impr. (%) | RV     | Impr. (%) |
| MNIST         | 5x100              | 0.0018                                     | 0.0005 | 233.96 ↑  | 0.0006 | 195.00 ↑  | 0.0006 | 216.07 ↑  |
|               | 3x700              | 0.0027                                     | 0.0008 | 251.28 ↑  | 0.0009 | 191.49 ↑  | 0.0009 | 191.49 ↑  |
|               | 3x400              | 0.0018                                     | 0.0007 | 166.67 ↑  | 0.0008 | 128.57 ↑  | 0.0007 | 137.84 ↑  |
|               | $\text{CNN}_{6-5}$ | 0.0243                                     | 0.0115 | 111.84 ↑  | 0.0131 | 85.94 ↑   | 0.0087 | 179.13 ↑  |
|               | 3x50               | 0.0012                                     | 0.0009 | 29.79 ↑   | 0.0010 | 27.08 ↑   | 0.0008 | 45.24 ↑   |
|               | $\text{CNN}_{3-4}$ | 0.0067                                     | 0.0055 | 21.05 ↑   | 0.0058 | 14.80 ↑   | 0.0055 | 20.83 ↑   |
|               | $\text{CNN}_{5-5}$ | 0.0108                                     | 0.0090 | 20.24 ↑   | 0.0092 | 17.50 ↑   | 0.0087 | 24.54 ↑   |
|               | $\text{CNN}_{4-5}$ | 0.0074                                     | 0.0061 | 21.21 ↑   | 0.0063 | 17.19 ↑   | 0.0060 | 23.63 ↑   |
| Fashion MNIST | 3x100              | 0.0156                                     | 0.0105 | 48.81 ↑   | 0.0110 | 42.04 ↑   | 0.0091 | 70.79 ↑   |
|               | $\text{CNN}_{4-5}$ | 0.0188                                     | 0.0134 | 41.12 ↑   | 0.0139 | 35.83 ↑   | 0.0129 | 45.82 ↑   |
|               | $\text{CNN}_{6-5}$ | 0.0329                                     | 0.0237 | 38.83 ↑   | 0.0242 | 35.67 ↑   | 0.0180 | 82.66 ↑   |
|               | 2x100              | 0.0109                                     | 0.0081 | 35.27 ↑   | 0.0085 | 28.59 ↑   | 0.0077 | 41.95 ↑   |
|               | 2x200              | 0.0102                                     | 0.0076 | 33.38 ↑   | 0.0080 | 27.06 ↑   | 0.0076 | 33.55 ↑   |
|               | $\text{CNN}_{5-5}$ | 0.0201                                     | 0.0153 | 31.52 ↑   | 0.0158 | 27.03 ↑   | 0.0125 | 60.69 ↑   |
| CIFAR10       | 3x200              | 0.0176                                     | 0.0083 | 113.30 ↑  | 0.0092 | 90.91 ↑   | 0.0080 | 119.40 ↑  |
|               | 3x50               | 0.0111                                     | 0.0073 | 53.52 ↑   | 0.0077 | 44.73 ↑   | 0.0071 | 56.32 ↑   |
|               | 3x100              | 0.0435                                     | 0.0243 | 78.79 ↑   | 0.0270 | 61.35 ↑   | 0.0256 | 69.66 ↑   |
|               | 3x400              | 0.0441                                     | 0.0245 | 79.67 ↑   | 0.0291 | 51.58 ↑   | 0.0253 | 74.69 ↑   |
|               | $\text{CNN}_{3-2}$ | 0.0106                                     | 0.0102 | 4.01 ↑    | 0.0102 | 4.01 ↑    | 0.0102 | 4.21 ↑    |
|               | $\text{CNN}_{3-4}$ | 0.0062                                     | 0.0061 | 1.80 ↑    | 0.0061 | 1.80 ↑    | 0.0061 | 1.96 ↑    |
|               | $\text{CNN}_{3-5}$ | 0.0066                                     | 0.0065 | 1.86 ↑    | 0.0065 | 1.86 ↑    | 0.0065 | 2.02 ↑    |

for the non-negative models. Nevertheless, the gradient-descent-based approach has been proven an efficient and practical solution to such convex optimization problems [17]. When the size of a network is reasonably small, such overhead is acceptable, compared with the improvement of the verification results.

**Experiment III.** Despite the infeasibility of network-wise tightest approximations in the general case (Section 3.3), we have explored the performance of our approximation method and the competitors on the networks of mixed weights. Table 5 shows the certified lower bounds returned by each approach for 11 CNNs and 9 FNNs.

First, the performance of each approach as compared with the others varies under different mixed-weight models. This coincides with our analysis in Section 3.3: Pure neuron-wise tightness does not imply a network-wise tightness. Moreover, we observe that our NEWISE performs surprisingly better than other approaches on all the experimented CNNs, while DEEPCERT and VERINET return larger certified lower bounds on the FNNs. The results evidenced network architecture is another factor influencing the verification. One possible reason is that a convolutional neural network is more possible to be monotonic based on the fact that the neurons' weights on the same layer are constrained to be identical [24].

Finally, we observe that average and standard deviation share the same increase/decrease trends. This indicates that a tighter approximation is more sensitive to the input images, which conforms to our conclusion in Experiment I.

### 6.3 Threats to Validity

We discuss potential threats to the validity of our approach in terms of its application domains.

**Neural Networks with ReLU Activation Functions.** Despite the focus on the Sigmoid-like activation functions, our approach is also applicable to the ReLU activation functions. A ReLU function  $\sigma(x) = \max(x, 0)$ , with  $x \in [l, u]$ , only needs approximation when

**Table 4: Performance comparison of Algorithm 1 with DEEPCERT (DC), VERINET (VN), and ROBUSTVERIFIER (RV) on 1-hidden-layer Sigmoid networks.  $t \times n$  refers to an FNN with  $t$  layers and  $n$  neurons per layer.  $\text{CNN}_{t-c-f}$  denotes a CNN with  $t$  layers and  $c$  filters of size  $f \times f$ . \* and + mark the models trained on MNIST and Fashion MNIST, respectively.**

| Arch. | Model                  | Certified Lower Bound (Standard Deviation) |        |           |        |           |        |           |
|-------|------------------------|--|--------|-----------|--------|-----------|--------|-----------|
|       |                        | Alg.1                                      | DC     | Impr. (%) | VN     | Impr. (%) | RV     | Impr. (%) |
| CNN   | $\text{CNN}_{2-1-5}^*$ | 0.0358                                     | 0.0145 | 146.32 ↑  | 0.0143 | 150.98 ↑  | 0.0137 | 160.66 ↑  |
|       | $\text{CNN}_{2-2-5}^*$ | 0.0308                                     | 0.0208 | 47.82 ↑   | 0.0207 | 48.96 ↑   | 0.0187 | 64.23 ↑   |
|       | $\text{CNN}_{2-3-5}^*$ | 0.0305                                     | 0.0197 | 54.80 ↑   | 0.0196 | 55.28 ↑   | 0.0176 | 73.57 ↑   |
|       | $\text{CNN}_{2-4-5}^*$ | 0.0419                                     | 0.0233 | 79.70 ↑   | 0.0232 | 80.56 ↑   | 0.0210 | 99.40 ↑   |
|       | $\text{CNN}_{2-5-3}^*$ | 0.0319                                     | 0.0182 | 75.22 ↑   | 0.0182 | 75.89 ↑   | 0.0176 | 81.59 ↑   |
|       | $\text{CNN}_{2-1-5}^+$ | 0.0497                                     | 0.0385 | 29.08 ↑   | 0.0386 | 28.74 ↑   | 0.0348 | 42.52 ↑   |
|       | $\text{CNN}_{2-2-5}^+$ | 0.0547                                     | 0.0353 | 54.77 ↑   | 0.0355 | 53.94 ↑   | 0.0311 | 75.66 ↑   |
|       | $\text{CNN}_{2-3-5}^+$ | 0.0541                                     | 0.0371 | 45.76 ↑   | 0.0374 | 44.71 ↑   | 0.0344 | 57.28 ↑   |
|       | $\text{CNN}_{2-4-5}^+$ | 0.0540                                     | 0.0366 | 47.48 ↑   | 0.0367 | 47.00 ↑   | 0.0336 | 60.41 ↑   |
|       | $\text{CNN}_{2-5-3}^+$ | 0.0598                                     | 0.0340 | 75.97 ↑   | 0.0340 | 75.71 ↑   | 0.0312 | 91.34 ↑   |
| FNN   | 1x50*                  | 0.0122                                     | 0.0082 | 49.16 ↑   | 0.0085 | 43.89 ↑   | 0.0062 | 96.32 ↑   |
|       | 1x100*                 | 0.0107                                     | 0.0064 | 67.67 ↑   | 0.0066 | 61.10 ↑   | 0.0050 | 114.80 ↑  |
|       | 1x150*                 | 0.0124                                     | 0.0083 | 50.17 ↑   | 0.0085 | 45.59 ↑   | 0.0064 | 93.75 ↑   |
|       | 1x200*                 | 0.0127                                     | 0.0074 | 71.99 ↑   | 0.0076 | 68.35 ↑   | 0.0058 | 120.58 ↑  |
|       | 1x250*                 | 0.0120                                     | 0.0075 | 60.93 ↑   | 0.0076 | 58.37 ↑   | 0.0060 | 100.82 ↑  |
|       | 1x50+                  | 0.0184                                     | 0.0117 | 56.83 ↑   | 0.0122 | 51.04 ↑   | 0.0089 | 107.35 ↑  |
|       | 1x100+                 | 0.0149                                     | 0.0119 | 25.06 ↑   | 0.0123 | 21.89 ↑   | 0.0088 | 70.46 ↑   |
|       | 1x150+                 | 0.0183                                     | 0.0120 | 52.83 ↑   | 0.0123 | 49.35 ↑   | 0.0090 | 103.61 ↑  |
|       | 1x200+                 | 0.0216                                     | 0.0129 | 67.41 ↑   | 0.0132 | 63.74 ↑   | 0.0096 | 125.31 ↑  |
|       | 1x250+                 | 0.0170                                     | 0.0126 | 34.67 ↑   | 0.0128 | 32.88 ↑   | 0.0095 | 77.96 ↑   |

$l < 0$  and  $u > 0$ ; the upper, resp. lower, linear bound would be then  $y = \frac{u}{u-l}(x-l)$ , resp.  $y = 0$ . Hence, the approximation is the tightest for non-negative neural networks. However, linear approximation is not a necessity for ReLU due to its piece-wise linearity. There are more precise (both sound and complete) verification approaches (by using, e.g., SMT [20] and Mixed Integer Linear Programming [6]) which could compute larger certified lower bounds.

**FNNs with Mixed Weights.** For such networks, it is generally unpredictable which approach would compute the most precise verification result (despite a 10% decrease on average in our approach). To the best of our knowledge, the only feasible way to examine a proposed approximation under non-trivial FNNs is by empirical analysis. Tackling this fundamentally and efficiently remains to be an open research problem.

## 7 RELATED WORK

This work is a sequel to many pioneering efforts, which we classify into the following three categories.

**Linear Approximations of Sigmoid-like activation functions.** NEVER [33] uses piece-wise linear constraints for approximation and is therefore unscalable. Both CROWN [55] and CNN-Cert [5] consider the tangent line at the midpoint of  $[l, u]$  as one of the linear bounds. DEEPCERT [51] defines a fine-grained approximation strategy by calculating the slopes of the two linear constraints according to  $l$  and  $u$ . ROBUSTVERIFIER [26] leverages Taylor expansion at the midpoint of  $[l, u]$ . These approximations are intuitive but lack rigorous justifications or proofs for their better performance.

Lyu *et al.* [28] characterized the tightness of approximations in terms of the overestimation of output range of each hidden neuron. But they observed and admitted that by their definition tighter bounding lines do not ensure more precise results. By our definition, we show that in the case of one hidden layer, their definition also

**Table 5: Performance comparison with DEEPCERT (DC), VERINET (VN), and ROBUSTVERIFIER (RV) on mixed-weights Sigmoid networks. \*, +, and # mark the models trained on MNIST, Fashion MNIST, and CIFAR10, respectively.**

| Arch.              | Model                           | #Neur.            | Certified Lower Bound |        |           |         |           |         |                    |        |        |           |         |           | Time (s) |          |              |
|--------------------|---------------------------------|-------------------|-----------------------|--------|-----------|---------|-----------|---------|--------------------|--------|--------|-----------|---------|-----------|----------|----------|--------------|
|                    |                                 |                   | Average               |        |           |         |           |         | Standard Deviation |        |        |           |         |           |          |          |              |
|                    |                                 |                   | NW                    | DC     | Impr. (%) | VN      | Impr. (%) | RV      | Impr. (%)          | NW     | DC     | Impr. (%) | VN      | Impr. (%) |          | RV       | Impr. (%)    |
| CNN                | CNN <sub>3_2</sub> <sup>*</sup> | 2,514             | 0.0607                | 0.0579 | 4.92 ↑    | 0.0580  | 4.67 ↑    | 0.0569  | 6.82 ↑             | 0.0219 | 0.0202 | 8.06 ↑    | 0.0204  | 7.37 ↑    | 0.0192   | 13.79 ↑  | 0.17 ±0.04   |
|                    | CNN <sub>3_4</sub> <sup>*</sup> | 5,018             | 0.0478                | 0.0472 | 1.17 ↑    | 0.0472  | 1.29 ↑    | 0.0464  | 2.95 ↑             | 0.0155 | 0.0153 | 1.11 ↑    | 0.0153  | 1.44 ↑    | 0.0146   | 5.87 ↑   | 0.31 ±0.08   |
|                    | CNN <sub>4_5</sub> <sup>*</sup> | 8,680             | 0.0570                | 0.0539 | 5.64 ↑    | 0.0543  | 5.03 ↑    | 0.0522  | 9.16 ↑             | 0.0157 | 0.0145 | 8.64 ↑    | 0.0146  | 7.52 ↑    | 0.0132   | 19.45 ↑  | 1.18 ±0.20   |
|                    | CNN <sub>5_5</sub> <sup>*</sup> | 10,680            | 0.0581                | 0.0548 | 6.06 ↑    | 0.0550  | 5.63 ↑    | 0.0512  | 13.42 ↑            | 0.0157 | 0.0142 | 10.48 ↑   | 0.0144  | 8.80 ↑    | 0.0120   | 30.81 ↑  | 2.99 ±0.38   |
|                    | CNN <sub>6_5</sub> <sup>*</sup> | 12,300            | 0.0624                | 0.0590 | 5.71 ↑    | 0.0588  | 6.00 ↑    | 0.0541  | 15.27 ↑            | 0.0171 | 0.0153 | 12.03 ↑   | 0.0153  | 11.96 ↑   | 0.0123   | 39.72 ↑  | 5.72 ±0.46   |
|                    | CNN <sub>8_5</sub> <sup>*</sup> | 14,570            | 0.1191                | 0.0878 | 35.58 ↑   | 0.0882  | 35.02 ↑   | 0.0685  | 73.75 ↑            | 0.0361 | 0.0248 | 45.60 ↑   | 0.0255  | 41.66 ↑   | 0.0163   | 122.22 ↑ | 15.27 ±0.78  |
|                    | CNN <sub>4_5</sub> <sup>+</sup> | 8,680             | 0.0747                | 0.0720 | 3.73 ↑    | 0.0720  | 3.79 ↑    | 0.0666  | 12.16 ↑            | 0.0413 | 0.0376 | 9.85 ↑    | 0.0378  | 9.12 ↑    | 0.0313   | 31.73 ↑  | 1.19 ±0.21   |
|                    | CNN <sub>5_5</sub> <sup>+</sup> | 10,680            | 0.0704                | 0.0676 | 4.14 ↑    | 0.0676  | 4.14 ↑    | 0.0605  | 16.51 ↑            | 0.0347 | 0.0318 | 9.03 ↑    | 0.0320  | 8.41 ↑    | 0.0244   | 41.82 ↑  | 2.99 ±0.40   |
|                    | CNN <sub>6_5</sub> <sup>+</sup> | 12,300            | 0.0735                | 0.0695 | 5.77 ↑    | 0.0691  | 6.37 ↑    | 0.0626  | 17.32 ↑            | 0.0368 | 0.0341 | 7.97 ↑    | 0.0340  | 8.35 ↑    | 0.0278   | 32.57 ↑  | 5.81 ±0.55   |
|                    | CNN <sub>3_2</sub> <sup>#</sup> | 3,378             | 0.0314                | 0.0312 | 0.58 ↑    | 0.0312  | 0.61 ↑    | 0.0311  | 1.06 ↑             | 0.0172 | 0.0169 | 1.65 ↑    | 0.0169  | 1.84 ↑    | 0.0168   | 2.69 ↑   | 0.31 ±0.06   |
|                    | CNN <sub>6_5</sub> <sup>#</sup> | 17,110            | 0.0229                | 0.0224 | 2.19 ↑    | 0.0223  | 2.46 ↑    | 0.0212  | 7.77 ↑             | 0.0158 | 0.0153 | 3.20 ↑    | 0.0153  | 3.20 ↑    | 0.0141   | 12.13 ↑  | 10.31 ±0.68  |
|                    | FNN                             | 3x50 <sup>*</sup> | 160                   | 0.0069 | 0.0076    | -8.82 ↓ | 0.0077    | -9.77 ↓ | 0.0065             | 6.62 ↑ | 0.0025 | 0.0027    | -6.37 ↓ | 0.0028    | -9.42 ↓  | 0.0021   | 18.48 ↑      |
| 3x100 <sup>*</sup> |                                 | 310               | 0.0078                | 0.0086 | -9.44 ↓   | 0.0087  | -10.79 ↓  | 0.0074  | 4.44 ↑             | 0.0026 | 0.0029 | -10.14 ↓  | 0.0029  | -12.88 ↓  | 0.0023   | 10.30 ↑  | 2.14 ±0.03   |
| 3x200 <sup>*</sup> |                                 | 610               | 0.0080                | 0.0091 | -11.69 ↓  | 0.0091  | -12.36 ↓  | 0.0079  | 1.01 ↑             | 0.0026 | 0.0030 | -14.14 ↓  | 0.0031  | -16.39 ↓  | 0.0024   | 5.37 ↑   | 10.77 ±0.01  |
| 5x100 <sup>*</sup> |                                 | 510               | 0.0057                | 0.0061 | -5.27 ↓   | 0.0062  | -6.66 ↓   | 0.0052  | 10.79 ↑            | 0.0024 | 0.0025 | -5.98 ↓   | 0.0026  | -8.88 ↓   | 0.0021   | 12.38 ↑  | 4.38 ±0.03   |
| 6x500 <sup>*</sup> |                                 | 3,010             | 0.0685                | 0.0778 | -11.95 ↓  | 0.0776  | -11.73 ↓  | 0.0665  | 3.05 ↑             | 0.0186 | 0.0210 | -11.56 ↓  | 0.0210  | -11.69 ↓  | 0.0152   | 21.98 ↑  | 154.39 ±0.36 |
| 3x50 <sup>+</sup>  |                                 | 160               | 0.0092                | 0.0101 | -9.67 ↓   | 0.0102  | -10.29 ↓  | 0.0086  | 6.64 ↑             | 0.0035 | 0.0037 | -6.74 ↓   | 0.0038  | -9.90 ↓   | 0.0030   | 15.72 ↑  | 0.14 ±0.00   |
| 5x100 <sup>+</sup> |                                 | 510               | 0.0071                | 0.0078 | -8.51 ↓   | 0.0079  | -10.01 ↓  | 0.0066  | 8.23 ↑             | 0.0036 | 0.0040 | -8.79 ↓   | 0.0041  | -11.68 ↓  | 0.0033   | 11.35 ↑  | 4.44 ±0.03   |
| 3x50 <sup>#</sup>  |                                 | 160               | 0.0041                | 0.0045 | -10.57 ↓  | 0.0045  | -10.18 ↓  | 0.0042  | -2.17 ↓            | 0.0018 | 0.0021 | -14.90 ↓  | 0.0021  | -14.49 ↓  | 0.0017   | 2.91 ↑   | 0.43 ±0.00   |
| 5x100 <sup>#</sup> |                                 | 510               | 0.0033                | 0.0037 | -10.60 ↓  | 0.0037  | -10.60 ↓  | 0.0033  | -0.60 ↓            | 0.0014 | 0.0017 | -15.06 ↓  | 0.0016  | -14.55 ↓  | 0.0013   | 5.22 ↑   | 2.45 ±0.01   |

guarantees to be network-wise tightest. They proposed a gradient-based searching algorithm for near-tightest approximations under their definition. However, the algorithm has been shown difficult to scale up to large-size networks because it needs to perform on every neuron, compared with other existing constant-time approaches [18, 51]. Our work is, to the best of our knowledge, the first provably tightest, constant-time linear approximation.

**Defining Tightness for Linear Approximations.** There has been a shift of focus from individual neurons to multiple neurons w.r.t. defining tightness for linear approximations, but most of the work only concerns about the ReLU networks. Tjandraatmadja *et al.* [41] experimentally show that the success of approximations hinges on how closely they approximate the object that they are relaxing. Salman *et al.* [36] reveal an inherent barrier of the approximation-based approaches for the ReLU networks and require for the tightest pre-activation upper and lower bounds of all the neurons in networks. Singh *et al.* [38] approximate multiple neurons simultaneously to obtain the tighter bounds. In contrast to this line of research, we have defined both neuron-wise and network-wise tightness to characterize linear approximations of Sigmoid-like activation functions.

**Other Robustness Verification Approaches.** In addition to approximation, other techniques have also been used for the robustness verification of neural networks. Abstract interpretation [11], a technique that was originally proposed for program verification, has been proven both effective and efficient in neural network verification [16, 39, 40]. These approaches also rely on over-approximation but to transform the original verification problem into dedicated abstract domains. We believe that our approximation approach is also applicable to produce more precise verification results for non-negative neural networks. Other verification methods leverage the Lipschitz continuity feature of neural networks to estimate the output ranges [10, 25, 35]. Although the approximation to an activation function can be bypassed using the Lipschitz constant, it would still be helpful to compute tighter Lipschitz constants by estimating the input range of the activation function via the approximation.

## 8 CONCLUDING REMARKS

We have presented *network-wise tightness*, a novel and unified characterization of the tightness of linear approximations in robustness verification of Sigmoid-like neural networks. We have shown that (i) to achieve precise verification results, activation functions in a network should *not* be approximated with the same existing neuron-wise tightness criterion; (ii) computing the network-wise tightest approximation is computationally expensive and impractical due to its non-convexity; and (iii) how to bypass the complexity barrier via a neuron-wise tightest approximation. The experimental results demonstrate that our approximation approach outperforms state-of-the-art approaches under three scenarios, i.e., non-negative networks, 1-hidden-layer networks, and convolutional networks.

Our work sheds light on the pursuit of robust neural networks via tightening linear approximations. The ineffectiveness of neuron-wise tightness on general networks calls for new, potentially hybrid, approximation strategies. The intrinsic high complexity in computing the network-wise tightest approximation motivates us to rethink of both fundamental and the heuristic trade-offs between precision and efficiency in neural network verification. For mixed-weight neural networks, there may be latent factors that could influence the tightness of approximations. One promising direction is to explore possible combinations of existing tightness characterizations to achieve network-wise tightness while taking into account the features of weight distributions and network architectures.

## ACKNOWLEDGMENTS

The authors thank the reviewers for their constructive comments. This work was supported in part by the National Key Research and Development (2019YFA0706404), the National Nature Science Foundation of China (61972150), the NSFC-ISF Joint Program (62161146001, 3420/21), the Fundamental Research Funds for Central Universities, and the Opening Project of Shanghai Trusted Industrial Control Platform. Jing Liu and Min Zhang are the corresponding authors.

## REFERENCES

- [1] Afan Ali and Fan Yangyu. 2017. Automatic modulation classification using deep learning based on sparse autoencoders with nonnegativity constraints. *IEEE signal processing letters* 24, 11 (2017), 1626–1630.
- [2] aptx4869tjx. 2021. Pretrained Models. [https://github.com/aptx4869tjx/train\\_network](https://github.com/aptx4869tjx/train_network).
- [3] Christel Baier and Joost-Pieter Katoen. 2008. *Principles of model checking*. MIT press.
- [4] Teodora Baluta, Zheng Leong Chua, Kuldeep S. Meel, and Prateek Saxena. 2021. Scalable Quantitative Verification For Deep Neural Networks. In *43rd IEEE/ACM International Conference on Software Engineering, ICSE 2021, Madrid, Spain, 22-30 May 2021*. IEEE, 312–323.
- [5] Akhilan Boopathy, Tsui-Wei Weng, Pin-Yu Chen, Sijia Liu, and Luca Daniel. 2019. CNN-Cert: An Efficient Framework for Certifying Robustness of Convolutional Neural Networks. In *AAAI Conference on Artificial Intelligence (AAAI)*, 3240–3247.
- [6] Elena Botoeva, Panagiotis Kouvaros, Jan Kronqvist, Alessio Lomuscio, and Ruth Misener. 2020. Efficient Verification of ReLU-Based Neural Networks via Dependency Analysis. In *AAAI Conference on Artificial Intelligence (AAAI)*. AAAI Press, 3291–3299.
- [7] Nicholas Carlini and David Wagner. 2017. Towards evaluating the robustness of neural networks. In *IEEE symposium on security and privacy (S&P)*. IEEE, 39–57.
- [8] Fabrício Ceschin, Marcus Botacin, Heitor Murilo Gomes, Luiz S Oliveira, and André Grégio. 2019. Shallow security: On the creation of adversarial variants to evade machine learning-based malware detectors. In *Proceedings of the 3rd Reversing and Offensive-oriented Trends Symposium*. 1–9.
- [9] Edmund M Clarke. 1997. Model checking. In *International Conference on Foundations of Software Technology and Theoretical Computer Science*. Springer, 54–56.
- [10] Patrick L Combettes and Jean-Christophe Pesquet. 2020. Lipschitz certificates for layered network structures driven by averaged activation operators. *SIAM Journal on Mathematics of Data Science* 2, 2 (2020), 529–557.
- [11] Patrick Cousot and Radhia Cousot. 1977. Abstract interpretation: a unified lattice model for static analysis of programs by construction or approximation of fixpoints. In *ACM Symposium on Principles of Programming Languages (POPL)*, 238–252.
- [12] Isaac Dunn, Hadrien Pouget, Daniel Kroening, and Tom Melham. 2021. Exposing previously undetectable faults in deep neural networks. In *30th ACM SIGSOFT International Symposium on Software Testing and Analysis (ISSTA)*. ACM, 56–66.
- [13] Souradeep Dutta, Susmit Jha, Sriram Sankaranarayanan, and Ashish Tiwari. 2018. Output Range Analysis for Deep Feedforward Neural Networks. In *NASA Formal Methods Symposium (NFM)*. Springer, 121–138.
- [14] Ruediger Ehlers. 2017. Formal verification of piece-wise linear feed-forward neural networks. In *International Symposium on Automated Technology for Verification and Analysis*. Springer, 269–286.
- [15] William Fleshman, Edward Raff, Jared Sylvester, et al. 2018. Non-Negative Networks Against Adversarial Attacks. *CoRR* abs/1806.06108 (2018). <http://arxiv.org/abs/1806.06108>
- [16] Timon Gehr, Matthew Mirman, Dana Drachler-Cohen, Petar Tsankov, Swarat Chaudhuri, and Martin Vechev. 2018. AI2: Safety and Robustness Certification of Neural Networks with Abstract Interpretation. In *IEEE Symposium on Security and Privacy (S&P)*. IEEE, 3–18.
- [17] Saad Hikmat Haji and Adnan Mohsin Abdulazeez. 2021. Comparison of optimization techniques based on gradient descent algorithm: A review. *PalArch's Journal of Archaeology of Egypt/Egyptology* 18, 4 (2021), 2715–2743.
- [18] Patrick Henriksen and Alessio R. Lomuscio. 2020. Efficient Neural Network Verification via Adaptive Refinement and Adversarial Search. In *European Conference on Artificial Intelligence (ECAI)*. IOS Press, 2513–2520.
- [19] Omid Kargarnovin, Amir Mahdi Sadeghzadeh, and Rasool Jalili. 2021. Mal2GCN: A Robust Malware Detection Approach Using Deep Graph Convolutional Networks With Non-Negative Weights. *arXiv preprint arXiv:2108.12473* (2021).
- [20] Guy Katz, Clark Barrett, David L Dill, Kyle Julian, and Mykel J Kochenderfer. 2017. Reluplex: An Efficient SMT Solver for Verifying Deep Neural Networks. In *International Conference on Computer Aided Verification (CAV)*. Springer, 97–117.
- [21] Alex Krizhevsky, Geoffrey Hinton, et al. 2009. Learning Multiple Layers of Features from Tiny Images. (2009).
- [22] Alex Krizhevsky, Ilya Sutskever, and Geoffrey E. Hinton. 2017. ImageNet classification with deep convolutional neural networks. *Commun. ACM* 60, 6 (2017), 84–90.
- [23] Yann LeCun, Léon Bottou, Yoshua Bengio, and Patrick Haffner. 1998. Gradient-Based Learning Applied to Document Recognition. *Proc. IEEE* 86, 11 (1998), 2278–2324.
- [24] Yann LeCun, Léon Bottou, Yoshua Bengio, and Patrick Haffner. 1998. Gradient-based learning applied to document recognition. *Proc. IEEE* 86, 11 (1998), 2278–2324.
- [25] Sungyoon Lee, Jaewook Lee, and Saerom Park. 2020. Lipschitz-certifiable training with a tight outer bound. *Annual Conference on Neural Information Processing Systems (NeurIPS)* 33 (2020), 16891–16902.
- [26] Wang Lin, Zhengfeng Yang, Xin Chen, Qingye Zhao, Xiangkun Li, Zhiming Liu, and Jifeng He. 2019. Robustness Verification of Classification Deep Neural Networks via Linear Programming. In *IEEE/CVF Conference on Computer Vision and Pattern Recognition (CVPR)*. 11418–11427.
- [27] Jonathan Long, Evan Shelhamer, and Trevor Darrell. 2015. Fully convolutional networks for semantic segmentation. In *IEEE/CVF Conference on Computer Vision and Pattern Recognition (CVPR)*. IEEE Computer Society, 3431–3440.
- [28] Zhaoyang Lyu, Ching-Yun Ko, Zhifeng Kong, Ngai Wong, Dahua Lin, and Luca Daniel. 2020. Fastened CROWN: Tightened Neural Network Robustness Certificates. In *AAAI Conference on Artificial Intelligence (AAAI)*. 5037–5044.
- [29] Ana Neacsu, Jean-Christophe Pesquet, and Corneliu Burileanu. 2020. Accuracy-Robustness Trade-Off for Positively Weighted Neural Networks. In *International Conference on Acoustics, Speech and Signal Processing (ICASSP)*. IEEE, 8389–8393.
- [30] Tianxiang Pan, Bin Wang, Guiguang Ding, and Jun-Hai Yong. 2017. Fully Convolutional Neural Networks with Full-Scale-Features for Semantic Segmentation. In *AAAI Conference on Artificial Intelligence (AAAI)*. AAAI Press, 4240–4246.
- [31] Harsh Nilesch Pathak and Randy Clinton Paffenroth. 2020. Non-convex Optimization Using Parameter Continuation Methods for Deep Neural Networks. *Deep Learning Applications, Volume 2* 1232 (2020), 273–298.
- [32] Brandon Paulsen, Jingbo Wang, Jiawei Wang, and Chao Wang. 2020. NEURODIFF: Scalable Differential Verification of Neural Networks using Fine-Grained Approximation. In *International Conference on Automated Software Engineering (ASE)*. IEEE, 784–796.
- [33] Luca Pulina and Armando Tacchella. 2010. An Abstraction-Refinement Approach to Verification of Artificial Neural Networks. In *International Conference on Computer Aided Verification (CAV)*. Springer, 243–257.
- [34] Shaoqing Ren, Kaiming He, Ross B. Girshick, and Jian Sun. 2017. Faster R-CNN: Towards Real-Time Object Detection with Region Proposal Networks. *IEEE Transactions on Pattern Analysis and Machine Intelligence* 39, 6 (2017), 1137–1149.
- [35] Wenjie Ruan, Xiaowei Huang, and Marta Kwiatkowska. 2018. Reachability analysis of deep neural networks with provable guarantees. In *International Joint Conference on Artificial Intelligence (IJCAI)*, 2651–2659.
- [36] Hadi Salman, Greg Yang, Huan Zhang, Cho-Jui Hsieh, and Pengchuan Zhang. 2019. A Convex Relaxation Barrier to Tight Robustness Verification of Neural Networks. In *Annual Conference on Neural Information Processing Systems (NeurIPS)*, 9832–9842.
- [37] Marco Sälzer and Martin Lange. 2021. Reachability Is NP-Complete Even for the Simplest Neural Networks. *CoRR* abs/2108.13179 (2021).
- [38] Gagandeep Singh, Rupanshu Ganvir, Markus Püschel, and Martin T. Vechev. 2019. Beyond the Single Neuron Convex Barrier for Neural Network Certification. In *Annual Conference on Neural Information Processing Systems (NeurIPS)*. 15072–15083.
- [39] Gagandeep Singh, Timon Gehr, Matthew Mirman, Markus Püschel, and Martin T Vechev. 2018. Fast and Effective Robustness Certification.. In *Advances in Neural Information Processing Systems (NeurIPS)*. 10825–10836.
- [40] Gagandeep Singh, Timon Gehr, Markus Püschel, and Martin Vechev. 2019. An Abstract Domain for Certifying Neural Networks. *Proceedings of the ACM on Programming Languages (POPL)* (2019), 1–30.
- [41] Christian Tjandraatmadja, Ross Anderson, Joey Huchette, Will Ma, Krunal Patel, and Juan Pablo Vielma. 2020. The Convex Relaxation Barrier, Revisited: Tightened Single-Neuron Relaxations for Neural Network Verification. In *Annual Conference on Neural Information Processing Systems (NeurIPS)*.
- [42] Vincent Tjeng, Kai Xiao, and Russ Tedrake. 2019. Evaluating Robustness of Neural Networks with Mixed Integer Programming. In *International Conference on Learning Representations (ICLR)*.
- [43] Alexander Toshev and Christian Szegedy. 2014. DeepPose: Human Pose Estimation via Deep Neural Networks. In *IEEE/CVF Conference on Computer Vision and Pattern Recognition (CVPR)*. IEEE Computer Society, 1653–1660.
- [44] Hoang-Dung Tran, Xiaodong Yang, Diego Manzananas Lopez, Patrick Musau, Luan Viet Nguyen, Weiming Xiang, Stanley Bak, and Taylor T Johnson. 2020. NNV: the neural network verification tool for deep neural networks and learning-enabled cyber-physical systems. In *International Conference on Computer Aided Verification (CAV)*. Springer, 3–17.
- [45] Shiqi Wang, Kexin Pei, Justin Whitehouse, Junfeng Yang, and Suman Jana. 2018. Efficient formal safety analysis of neural networks. In *Annual Conference on Neural Information Processing Systems (NeurIPS)*. 6369–6379.
- [46] Shiqi Wang, Kexin Pei, Justin Whitehouse, Junfeng Yang, and Suman Jana. 2018. Formal Security Analysis of Neural Networks using Symbolic Intervals. In *USENIX Security Symposium (USENIX Security)*. 1599–1614.
- [47] Shiqi Wang, Huan Zhang, Kaidi Xu, Xue Lin, Suman Jana, Cho-Jui Hsieh, and J Zico Kolter. 2021. Beta-crown: Efficient bound propagation with per-neuron split constraints for neural network robustness verification. *Annual Conference on Neural Information Processing Systems (NeurIPS)* 34 (2021).
- [48] Lily Weng, Huan Zhang, Hongge Chen, Zhao Song, et al. 2018. Towards Fast Computation of Certified Robustness for ReLU Networks. In *International Conference on Machine Learning (ICML)*. PMLR, 5276–5285.
- [49] Tsui-Wei Weng, Huan Zhang, Hongge Chen, Zhao Song, et al. 2018. Towards Fast Computation of Certified Robustness for ReLU Networks. In *International*

- Conference on Machine Learning* ICML, Vol. 80. PMLR, 5273–5282.
- [50] Jeannette M Wing. 2021. Trustworthy AI. *Commun. ACM* 64, 10 (2021), 64–71.
- [51] Yiting Wu and Min Zhang. 2021. Tightening Robustness Verification of Convolutional Neural Networks with Fine-Grained Linear Approximation. In *AAAI Conference on Artificial Intelligence (AAAI)*. 11674–11681.
- [52] Weiming Xiang, Hoang-Dung Tran, and Taylor T Johnson. 2018. Output reachable set estimation and verification for multilayer neural networks. *IEEE transactions on neural networks and learning systems* 29, 11 (2018), 5777–5783.
- [53] Han Xiao, Kashif Rasul, and Roland Vollgraf. 2017. Fashion-MNIST: a Novel Image Dataset for Benchmarking Machine Learning Algorithms. *CoRR* abs/1708.07747 (2017).
- [54] Ming Yan, Junjie Chen, Xiangyu Zhang, Lin Tan, Gan Wang, and Zan Wang. 2021. Exposing numerical bugs in deep learning via gradient back-propagation. In *29th ACM Joint European Software Engineering Conference and Symposium on the Foundations of Software Engineering (ESEC/FSE)*. ACM, 627–638.
- [55] Huan Zhang, Tsui-Wei Weng, Pin-Yu Chen, Cho-Jui Hsieh, and Luca Daniel. 2018. Efficient Neural Network Robustness Certification with General Activation Functions. In *Annual Conference on Neural Information Processing Systems (NeurIPS)*. 4944–4953.
- [56] Zhaodi Zhang, Yitinh Wu, Si Liu, Jing Liu, and Min Zhang. 2022. *Provably Tightest Linear Approximation for Robustness Verification of Sigmoid-like Neural Networks*. Technical Report. <https://arxiv.org/abs/2208.09872>